Optimal Multi-View Video Transmission in Multiuser Wireless Networks by Exploiting Natural and View Synthesis-Enabled Multicast Opportunities

Wei Xu, Ying Cui, *Member, IEEE*, and Zhi Liu, *Member, IEEE*

***Abstract*— Multi-view videos (MVVs) provide immersive viewing experience, at the cost of traffic load increase for wireless networks. In this paper, we would like to optimize MVV transmission in a multiuser wireless network by exploiting both natural multicast opportunities and view synthesis-enabled multicast opportunities. Specifically, we first establish a mathematical model to specify view synthesis at the server and each user, and characterize its impact on multicast opportunities. This model is highly nontrivial and fundamentally enables the optimization of view synthesis-based multicast opportunities. For given video quality requirements of all users, we consider the optimization of view selection, transmission time and power allocation to minimize the average weighted sum energy consumption for view transmission and synthesis. In addition, under the energy consumption constraints at the server and each user respectively, we consider the optimization of view selection, transmission time and power allocation and video quality selection to maximize the total utility. These two optimization problems are challenging mixed discrete-continuous optimization problems. For the first problem, we propose an algorithm to obtain an optimal solution with reduced computational complexity by exploiting optimality properties. For each problem, to reduce computational complexity, we also propose a low-complexity algorithm to obtain a suboptimal solution, using Difference of Convex (DC) programming. Finally, numerical results show the advantage of the proposed solutions over existing ones, and demonstrate the importance of the optimization of view synthesis-enabled multicast opportunities in MVV transmission.**

***Index Terms*— Multi-view video, view synthesis, multicast, convex optimization, DC programming.**

I. Introduction

A MULTI-VIEW video (MVV) is generated by capturing a scene of interest with multiple cameras from different angles simultaneously. Each camera can capture both texture maps (i.e., images) and depth maps (i.e., distances from objects in the scene), providing one view. Besides views captured by cameras, additional views, providing new view angles, can be synthesized based on reference views using Depth-Image-Based Rendering (DIBR) [2]. A MVV subscriber (i.e., user) can freely select among multiple view angles, hence enjoying immersive viewing experience. MVV is one key technique in free-viewpoint television, naked-eye 3D and virtual reality (VR) [3], [4]. Thus, it has vast applications in entertainment, education, medicine, etc. The global market of VR related products is predicted to reach 30 billion USD by 2020 [5].

A MVV is in general of a much larger size than a traditional single-view video, bringing a heavy burden to wireless networks. Multiple views of a MVV can be jointly encoded using multiview video coding [6], [7] or separately encoded using state-of-the-art codec such as H.264/AVC and HEVC [8]. In particular, joint encoding achieves a significant coding gain by exploiting statistical dependencies from both temporal and inter-view reference frames for motion-compensated prediction [9]–[12]. However, it yields a great traffic load causing bandwidth waste. This is because with joint encoding, multiple views have to be delivered simultaneously to a user even though most of them will not be utilized by the user. To improve transmission efficiency, views are usually encoded separately at the cost of coding efficiency, and transmitted on demand [13]–[16]. In this paper, we restrict our attention to MVV transmission based on separate encoding.

In [14]–[17], the authors consider a wired MVV system with a single server and multiple users. In particular, [14], [16], [17] consider view synthesis only at the users, while [15] considers view synthesis both at the server and users. Note that view synthesis usually introduces distortion, the degree of which depends on the distance between the synthesized view and each of its two reference views and the qualities of the two reference views. Thus, in [14]–[17], view selection is optimized to minimize the total distortion of all synthesized views subject to the bandwidth constraint. The transmission models in [14]–[17] do not reflect channel fading and broadcast nature which are key features of wireless networks. Thus, the solutions for MVV transmission in [14]–[17] cannot be directly applied to MVV transmission in multiuser wireless networks.

Manuscript received April 10, 2019; revised August 20, 2019 and November 2, 2019; accepted November 14, 2019. Date of publication November 20, 2019; date of current version March 18, 2020. The work of Y. Cui was supported in part by NSFC China (61771309, 61671301, 61420106008, 61521062). The work of Z. Liu was supported by JSPS KAKENHI grants 18K18036, 19H04092, and The Telecommunications Advancement Foundation Research Fund. This article was presented in part at the IEEE GLOBECOM 2018 [1]. The associate editor coordinating the review of this article and approving it for publication was A. Cohen. *(Corresponding author: Ying Cui.)*

W. Xu and Y. Cui are with the Department of Electronic Engineering, Shanghai Jiao Tong University, Shanghai 200240, China (e-mail: cuiying@sjtu.edu.cn).

Z. Liu is with the Department of Mathematical and Systems Engineering, Shizuoka University, Hamamatsu 432-8561, Japan (e-mail: liu@ieee.org).

Color versions of one or more of the figures in this article are available online at http://ieeexplore.ieee.org.

Digital Object Identifier 10.1109/TCOMM.2019.2954523

In [18]–[21], the authors consider a wireless MVV transmission system with a single server [18]–[20] or multiple servers [21] and multiple users, where channel fading and broadcast nature of wireless communications are captured. The transmission mechanisms in [18]–[21] make use of natural multicast opportunities to reduce energy consumption. In particular, [18], [19], [21] consider Orthogonal Frequency Division Multiple Access (OFDMA), and optimize power and subcarrier allocation to minimize the total transmission power [18], [19] or bandwidth consumption [21]. None of [18], [19] and [21] considers view synthesis at the server or users, which can create multicast opportunities to further improve transmission efficiency in multiuser wireless networks. Thus, the transmission designs in [18], [19] and [21] may be further improved. In [20], the authors adopt view synthesis at each user to create multicast opportunities, but do not consider view synthesis at the server, and hence the transmission design in [20] cannot optimally utilize view synthesis-enabled multicast opportunities.

In this paper, we would like to address the above limitations. We consider MVV transmission from a server to multiple users in a wireless network with Time Division Multiple Access (TDMA) for multiple views. Different from [18], [19], [21], we allow view synthesis at the server and each user to maximally create multicast opportunities for efficient MVV transmission in multiuser wireless networks. The main contributions of this paper are summarized below.[1]

- First, we establish a mathematical model to specify view synthesis at the server and each user and characterize its impact on multicast opportunities. Note that this model is highly nontrivial and fundamentally enables the optimization of multicast opportunities. To the best of our knowledge, this is the first work providing an elegant mathematical model for specifying and controlling view synthesis at the server and all users.
- Then, we consider the optimization of view selection, transmission time and power allocation to minimize the average weighted sum energy consumption for view transmission and synthesis, for given quality requirements of all users. The problem is a challenging mixed discrete-continuous optimization problem. We propose an algorithm to obtain an optimal solution with reduced computational complexity, by exploiting optimality properties of the problem. To further reduce computational complexity, we propose a low-complexity algorithm to obtain a suboptimal solution, by transforming the original problem into a Difference of Convex (DC) problem and obtaining a stationary point of it using a DC algorithm.
- Next, we consider the optimization of view selection, transmission time and power allocation and quality selection to maximize the total utility under the energy consumption constraints for the server and each user, respectively. The problem is more challenging, as it has extra discrete variables and the constraint functions are not tractable. By using equivalent transformations and DC programming, we propose a low-complexity algorithm to obtain a suboptimal solution.
- Finally, numerical results show that the proposed solutions provide substantial gains compared to existing solutions, and demonstrate the importance of the optimization of view synthesis-enabled multicast opportunities in MVV transmission.

The key notation used in this paper is listed in Table I.

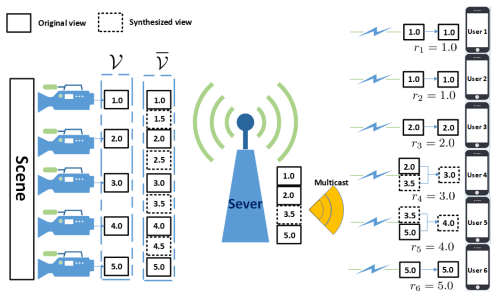

Fig. 1. System model. $K=6$, $r_1=1$, $r_2=1$, $r_3=2$, $r_4=3$, $r_5=4$, $r_6=5$, $V=5$, $\mathcal{V}=\{1,2,3,4,5\}$, $\overline{\mathcal{V}}=\{1,1.5,2,\cdots,5\}$, $\Delta_k=1$ for all $k\in\mathcal{K}$, $x_1=x_2=x_{3.5}=x_5=1$ and $y_{1,1}=y_{2,1}=y_{3,2}=y_{4,2}=y_{4,3.5}=y_{5,3.5}=y_{5,5}=y_{6,5}=1$.

II. System Model

As illustrated in Fig. 1, we consider downlink transmission of a MVV from a single-antenna server (e.g., base station or access point) to K (>1) single-antenna users, denoted by set $\mathcal{K}\triangleq\{1,2,\cdots,K\}$. V (>1) views (including texture maps and depth maps) about a scene of interest, denoted by set $\mathcal{V}\triangleq\{1,2,\cdots,V\}$, are captured by V evenly spaced cameras simultaneously from different view angles, and are referred to as the original views. The V original views are then pre-encoded independently using standard video codec and stored at the server. We consider $Q-1$ evenly spaced additional views between original view v and original view $v+1$, where $Q=2,3,\cdots$ is a system parameter and $v\in\{1,2,\cdots,V-1\}$. That is, the view spacing between any two neighboring views is $1/Q$. The additional views, providing new view angles, can be synthesized via DIBR. The set of indices for all views, including the V original views (which are stored at the server) and the $(V-1)(Q-1)$ additional views (which are not stored at the server but can be synthesized at the server), is denoted by $\overline{\mathcal{V}}\triangleq\{1,1+1/Q,1+2/Q,\cdots,V\}$. For ease of exposition, we assume all views have the same source encoding rate, denoted by R (in bit/s).

Using DIBR, a view can be synthesized using one left view and one right view as the reference views, at the server or a user. The quality of each synthesized view depends on its distance to its two reference views and the qualities. The server may need to synthesize any additional view $v\in\overline{\mathcal{V}}\setminus\mathcal{V}$ as it stores only the original views. Specifically, it can synthesize additional view $v\in\overline{\mathcal{V}}\setminus\mathcal{V}$ using its nearest left original view $\lfloor v\rfloor$ and right original view $\lceil v\rceil$.[2] Each user k may need to synthesize any view $v\in\overline{\mathcal{V}}\setminus\{1,V\}$,[3] using two views from the left reference view set $\overline{\mathcal{V}}_{k,v}^{-}\triangleq\{x\in\overline{\mathcal{V}}:v-\Delta_k\le x<v\}$ and

[1]This paper extends the results in the conference version [1] which does not consider the difference in timescale between view selection and time and power allocation, and studies only the energy consumption minimization problem.

[2]$\lfloor v\rfloor$ denotes the greatest integer less than or equal to v, and $\lceil v\rceil$ denotes the least integer greater than or equal to v.

[3]Note that view 1 and view V cannot be synthesized as they are boundary views.

TABLE I
KEY NOTATION

Notation	Description
$\mathcal{V}$	set of original views
$\overline{\mathcal{V}}$	set of all views
$\mathcal{K}$	set of all users
R	source encoding rate of all views
$\mathcal{H}$	finite channel state space
Δ_k	maximum allowable distance between synthesized view and two reference views for user k
r_k	view requested by user k
$x_v \in \{0,1\}$	view transmission variable for view v
$y_{k,v} \in \{0,1\}$	view utilization variable for view v at user k
$t_{\mathbf{h},v} \geq 0$	time allocated to transmit view v under system channel state $\mathbf{h}$
$p_{\mathbf{h},v} \geq 0$	power allocated to transmit view v under system channel state $\mathbf{h}$
E_b	synthesis energy consumption per time slot for one view at server
$E_{\mathrm{u},k}$	synthesis energy consumption per time slot for one view at user k
R	source encoding rate of all views
T	slot duration
B	bandwidth

the right reference view set $\overline{\mathcal{V}}^+_{k,v} \triangleq \{x \in \overline{\mathcal{V}} : v < x \leq v+\Delta_k\}$, respectively, where

$$\Delta_k \in \{1, 1+1/Q, \cdots, V-1\}, \quad k \in \mathcal{K}. \tag{1}$$

Here, Δ_k denotes the maximum allowable distance between any synthesized view and each of its two reference views for user k. Thus, Δ_k can reflect the view quality for user k. That is, a smaller Δ_k indicates higher quality for user k.

Let $U_k(\Delta_k)$ denote the utility of user k for view quality Δ_k, where $U_k(\cdot)$ can be an arbitrary nonnegative, strictly decreasing and concave function [22]. Then, for given qualities $\mathbf{\Delta} \triangleq (\Delta_k)_{k\in\mathcal{K}}$, the total utility is given by

$$U(\mathbf{\Delta}) \triangleq \sum_{k\in\mathcal{K}} U_k(\Delta_k). \tag{2}$$

We study the system for the duration of the playback time of multiple groups of pictures (GOPs), and assume that the view angle of each user does not change within the considered duration. Note that the playback time of one GOP is usually 0.5–1 seconds. Let $r_k \in \overline{\mathcal{V}}$ denote the index of the view requested by user $k \in \mathcal{K}$. Assume $r_k, k \in \mathcal{K}$ are known at the server. To satisfy user k's view request, if $r_k \in \overline{\mathcal{V}} \setminus \{1, V\}$, the server transmits either view r_k or two reference views in $\overline{\mathcal{V}}^-_{k,r_k}$ and $\overline{\mathcal{V}}^+_{k,r_k}$, respectively, for user k to synthesize view r_k; if $r_k \in \{1, V\}$, the server transmits view r_k. To save transmission resource by making use of multicast opportunities, the server transmits each view at most once.

Let x_v denote the view transmission variable for view v, where

$$x_v \in \{0,1\}, \quad v \in \overline{\mathcal{V}}. \tag{3}$$

Here, $x_v = 1$ indicates that the server will transmit view v and $x_v = 0$ otherwise. Denote $\mathbf{x} \triangleq (x_v)_{v\in\overline{\mathcal{V}}}$. As for all $v \in \overline{\mathcal{V}} \setminus \mathcal{V}$, $x_v = 1$ indicates that view v is synthesized at the server, $\mathbf{x}$ also reflects view synthesis at the server. Let $y_{k,v}$ denote the view utilization variable for view v at user k, where

$$y_{k,v} \in \{0,1\}, \quad v \in \overline{\mathcal{V}},\ k \in \mathcal{K}. \tag{4}$$

Here, $y_{k,v} = 1$ indicates that user k will utilize view v (as view v is requested by user k, i.e., $r_k = v$, or view $v \in \overline{\mathcal{V}}^-_{k,r_k} \cup \overline{\mathcal{V}}^+_{k,r_k}$ will be used to synthesize view r_k at user k) and $y_{k,v} = 0$ otherwise. It is clear that $\mathbf{y} \triangleq (y_{k,v})_{k\in\mathcal{K},v\in\overline{\mathcal{V}}}$ reflects view synthesis at all users. To guarantee that each user can obtain its requested view, we require:[4]

$$y_{k,r_k} + \sum_{v\in\overline{\mathcal{V}}^+_{k,r_k}} y_{k,v} = 1, \quad k \in \mathcal{K}, \tag{5}$$

$$y_{k,r_k} + \sum_{v\in\overline{\mathcal{V}}^-_{k,r_k}} y_{k,v} = 1, \quad k \in \mathcal{K}, \tag{6}$$

$$\sum_{v\in\overline{\mathcal{V}}\setminus(\{r_k\}\cup\overline{\mathcal{V}}^-_{k,r_k}\cup\overline{\mathcal{V}}^+_{k,r_k})} y_{k,v} = 0, \quad k \in \mathcal{K}. \tag{7}$$

Note that the constraints in (4), (5) and (6) indicate that user k either utilizes view r_k directly, i.e.,

$$y_{k,r_k} = 1,\ y_{k,v} = 0, \quad v \in \overline{\mathcal{V}}^-_{k,r_k} \cup \overline{\mathcal{V}}^+_{k,r_k},\ k \in \mathcal{K},$$

or utilizes one left view in $\overline{\mathcal{V}}^-_{k,r_k}$ and one right view in $\overline{\mathcal{V}}^+_{k,r_k}$ to synthesize view r_k, i.e.,

$$y_{k,r_k} = 0, \sum_{v\in\overline{\mathcal{V}}^-_{k,r_k}} y_{k,v} = \sum_{v\in\overline{\mathcal{V}}^+_{k,r_k}} y_{k,v} = 1,\ k \in \mathcal{K}.$$

In addition, the constraints in (4) and (7) indicate that user k does not utilize view r_k or views that are not in its two reference view sets, i.e.,

$$y_{k,v} = 0, \quad v \in \overline{\mathcal{V}} \setminus (\{r_k\} \cup \overline{\mathcal{V}}^-_{k,r_k} \cup \overline{\mathcal{V}}^+_{k,r_k}),\ k \in \mathcal{K}.$$

The server has to transmit view v in order for a user to utilize view v. Thus, we have the following constraints on the relation between the view transmission variables and view utilization variables:

$$x_v \geq y_{k,v}, \quad k \in \mathcal{K},\ v \in \overline{\mathcal{V}}. \tag{8}$$

We also refer to $(\mathbf{x}, \mathbf{y})$ as view selection variables, as we can control view synthesis at the server and all users via choosing values for $(\mathbf{x}, \mathbf{y})$. Due to the video coding structure, we do not allow the change of values for $(\mathbf{x}, \mathbf{y})$ during the considered time duration.

[4]For notation simplicity, for all $k \in \mathcal{K}$, we define $\sum_{v\in\overline{\mathcal{V}}^-_{k,r_k}} y_{k,v} = 0$ if $\overline{\mathcal{V}}^-_{k,r_k} = \emptyset$ and $\sum_{v\in\overline{\mathcal{V}}^+_{k,r_k}} y_{k,v} = 0$ if $\overline{\mathcal{V}}^+_{k,r_k} = \emptyset$.

The following example shows how view selection variables $(\mathbf{x}, \mathbf{y})$ affect multicast opportunities.

Example 1 (Natural and View Synthesis-Enabled Multicast Opportunities): Consider an illustration example as shown in Fig. 1. Consider $K = 6$, $r_1 = 1$, $r_2 = 1$, $r_3 = 2$, $r_4 = 3$, $r_5 = 4$, $r_6 = 5$, $V = 5$, $\mathcal{V} = \{1, 2, 3, 4, 5\}$, $\overline{\mathcal{V}} = \{1, 1.5, 2, \cdots, 5\}$ and $\Delta_k = 1$ for all $k \in \mathcal{K}$. As user 1 and user 2 both request view 1, view 1 can be transmitted once to serve the two users simultaneously, corresponding to natural multicast opportunities. Without view synthesis, the server has to transmit five views, i.e., views 1, 2, 3, 4 and 5 (with view 1 being utilized by two users), making use of natural multicast opportunities. In contrast, if view synthesis is allowed at the server and each user, the server transmit only four views, i.e., views 1, 2, 3.5 and 5 (each being utilized by two users), utilizing both natural and view synthesis-enabled multicast opportunities.

Based on view selection variables $(\mathbf{x}, \mathbf{y})$, the proposed model mathematically specifies view synthesis at the sever and all users, and characterizes its impact on multicast opportunities. Later, we shall see that this enables the optimization of multicast opportunities.

We consider a slotted narrowband system of bandwidth B (in Hz). Consider the block fading channel model, i.e., assume the channel of each user does not change within one time slot of duration T (in seconds). Note that T is about 0.005 seconds. For an arbitrary time slot, let $H_k \in \mathcal{H}$ denote the random channel state of user k, representing the power of the channel between user k and the server, where $\mathcal{H}$ denotes the finite[5] channel state space. Let $\mathbf{H} \triangleq (H_k)_{k\in\mathcal{K}} \in \mathcal{H}^K$ denote the random system channel state at an arbitrary time slot, where $\mathcal{H}^K$ represents the finite system channel state space. We assume that the server is aware of the system channel state $\mathbf{H}$ at each time slot. Suppose that the random system channel states over time slots are i.i.d. The probability of the random system channel state $\mathbf{H}$ at each time slot being $\mathbf{h} \triangleq (h_k)_{k\in\mathcal{K}} \in \mathcal{H}^K$ is given by $q_{\mathbf{H}}(\mathbf{h}) \triangleq \Pr[\mathbf{H} = \mathbf{h}]$.

We consider Time Division Multiple Access (TDMA)[6] for multiple views. That is, different views are transmitted one after another over the same frequency channel. Consider an arbitrary time slot. The time allocated to transmit view v under the system channel state $\mathbf{h}$, denoted by $t_{\mathbf{h},v}$, satisfies:

$$t_{\mathbf{h},v} \geq 0, \quad \mathbf{h} \in \mathcal{H}^K, \ v \in \overline{\mathcal{V}}. \tag{9}$$

In addition, we have the following total time allocation constraints under the system channel state $\mathbf{h}$:

$$\sum_{v\in\overline{\mathcal{V}}} t_{\mathbf{h},v} \leq T, \quad \mathbf{h} \in \mathcal{H}^K. \tag{10}$$

The transmission power for view v under the system channel state $\mathbf{h}$, denoted by $p_{\mathbf{h},v}$, satisfies:

$$p_{\mathbf{h},v} \geq 0, \quad \mathbf{h} \in \mathcal{H}^K, \ v \in \overline{\mathcal{V}}. \tag{11}$$

[5]Note that we consider a finite channel state space for tractability of optimization. In addition, note that due to limited accuracy for channel estimation (and channel feedback), the operational channel state space in practical systems is finite.

[6]Note that TDMA is analytically tractable and has applications in WiFi systems. In addition, the proposed transmission scheme and the optimization framework for a TDMA system can be extended to an OFDMA system [23].

The maximum transmission rate of view v to user k under the system channel state $\mathbf{h}$ is given by $\frac{Bt_{\mathbf{h},v}}{T}\log_2\left(1+\frac{p_{\mathbf{h},v}h_k}{\sigma^2}\right)$ (in bits/s), where σ^2 is the power (in Watt) of the complex additive white Gaussian channel noise at each receiver. To reduce the chance of stall (i.e., the chance that a playback buffer is empty) during the video playback at each user, the average arrival rate of each playback queue should be no less than its service rate. Thus, we have the following successful transmission constraints:[7]

$$\frac{B}{T}\mathbb{E}_{\mathbf{H}}\left[t_{\mathbf{H},v}\log_2\left(1+\frac{p_{\mathbf{H},v}H_k}{\sigma^2}\right)\right] \geq y_{k,v}R, \quad k \in \mathcal{K}, \ v \in \overline{\mathcal{V}}, \tag{12}$$

where the expectation $\mathbb{E}_{\mathbf{H}}$ is taken over the random system channel state $\mathbf{H} \in \mathcal{H}^K$. The transmission energy consumption per time slot under the system channel state $\mathbf{h}$ at the server is $\sum_{v\in\overline{\mathcal{V}}} t_{\mathbf{h},v}p_{\mathbf{h},v}$. Besides view transmission, view synthesis also consumes energy. For ease of exposition, we assume that the energy consumptions for synthesizing different views at the server are the same. Let E_b denote the synthesis energy consumption (in Joule) [24] per time slot for one view at the server. Thus, the total synthesis energy consumption per time slot at the server is $\sum_{v\in\overline{\mathcal{V}}\setminus\mathcal{V}} x_v E_b$. Let $E_{\mathrm{u},k}$ denote the synthesis energy consumption (in Joule) per time slot for one view at user k. Considering heterogeneous hardware conditions at different users, we allow $E_{\mathrm{u},k}, k \in \mathcal{K}$ to be different. Then, the synthesis energy consumption per time slot at user k is $(1-y_{k,r_k})E_{\mathrm{u},k}$, and the total synthesis energy consumption per time slot at all users is $\sum_{k\in\mathcal{K}}(1-y_{k,r_k})E_{\mathrm{u},k}$. Therefore, the weighted sum energy consumption per time slot under the system channel state $\mathbf{h}$ is given by:

$$\begin{aligned} E(\mathbf{x}, \mathbf{y}, \mathbf{t_h}, \mathbf{p_h}) = &\sum_{v\in\overline{\mathcal{V}}} t_{\mathbf{h},v}p_{\mathbf{h},v} + \sum_{v\in\overline{\mathcal{V}}\setminus\mathcal{V}} x_v E_b \\ &+\beta\sum_{k\in\mathcal{K}}(1-y_{k,r_k})E_{\mathrm{u},k}, \quad \mathbf{h} \in \mathcal{H}^K, \end{aligned} \tag{13}$$

where $\mathbf{x} \triangleq (x_v)_{v\in\overline{\mathcal{V}}}$, $\mathbf{y} \triangleq (y_{k,v})_{k\in\mathcal{K},v\in\overline{\mathcal{V}}}$, $\mathbf{t_h} \triangleq (t_{\mathbf{h},v})_{v\in\overline{\mathcal{V}}}$, $\mathbf{p_h} \triangleq (p_{\mathbf{h},v})_{v\in\overline{\mathcal{V}}}$ and $\beta \geq 1$ is the corresponding weight factor for the K users. Note that $\beta > 1$ means imposing a higher cost on the energy consumptions for user devices due to their limited battery powers. The average weighted sum energy consumption per time slot is given by

$$\begin{aligned} \mathbb{E}_{\mathbf{H}}[E(\mathbf{x}, \mathbf{y}, \mathbf{t_H}, \mathbf{p_H})] = &\mathbb{E}_{\mathbf{H}}\left[\sum_{v\in\overline{\mathcal{V}}} t_{\mathbf{H},v}p_{\mathbf{H},v}\right] + \sum_{v\in\overline{\mathcal{V}}\setminus\mathcal{V}} x_v E_b \\ &+\beta\sum_{k\in\mathcal{K}}(1-y_{k,r_k})E_{\mathrm{u},k}. \end{aligned} \tag{14}$$

In Section III, we shall minimize the average weighted sum energy consumption for given quality requirements of all users. In Section IV, we shall maximize the total utility under the energy consumption constraints at the server and each user.

[7]More conservatively, we can use $R + \delta$ for some $\delta > 0$ in (12) instead of R. In addition, in the startup phase, the playback buffer usually stores some view data, say L_0 bits. It is known that the chance of stall during the playback phase decreases with δ and with L_0.

III. Average Weighted Sum Energy Minimization

In this section, we consider the minimization of the average weighted sum energy consumption for given quality requirements of all users. We first formulate the optimization problem. Then, we develop an algorithm to obtain an optimal solution with reduced computational complexity by exploiting optimality properties. Finally, to further reduce computational complexity, we develop a low-complexity algorithm to obtain a suboptimal solution using DC programming.

A. Problem Formulation

We would like to minimize the average weighted sum energy consumption by optimizing the view selection and transmission time and power allocation for given quality requirements of all users. Specifically, for given $\mathbf{\Delta}$, we have the following optimization problem.

Problem 1 (Energy Minimization):

$$\begin{aligned} E^\star \triangleq \min_{\mathbf{x},\mathbf{y},\mathbf{t},\mathbf{p}} \quad & \mathbb{E}_{\mathbf{H}}\left[E(\mathbf{x},\mathbf{y},\mathbf{t}_{\mathbf{H}},\mathbf{p}_{\mathbf{H}})\right] \\ \text{s.t.} \quad & (3),(4),(5),(6),(7),(8),(9),(10),(11),(12), \end{aligned}$$

where $\mathbb{E}_{\mathbf{H}}[E(\mathbf{x},\mathbf{y},\mathbf{t}_{\mathbf{H}},\mathbf{p}_{\mathbf{H}})]$ is given by (14). Let $(\mathbf{x}^\star,\mathbf{y}^\star,\mathbf{t}^\star,\mathbf{p}^\star)$ denote an optimal solution of Problem 1, where $\mathbf{x}^\star \triangleq (x_v^\star)_{v\in\overline{\mathcal{V}}}$, $\mathbf{y}^\star \triangleq (y_{k,v}^\star)_{k\in\mathcal{K},v\in\overline{\mathcal{V}}}$, $\mathbf{t}^\star \triangleq (t_{\mathbf{h},v}^\star)_{\mathbf{h}\in\mathcal{H}^K,v\in\overline{\mathcal{V}}}$ and $\mathbf{p}^\star \triangleq (p_{\mathbf{h},v}^\star)_{\mathbf{h}\in\mathcal{H}^K,v\in\overline{\mathcal{V}}}$.

Problem 1 is a challenging mixed discrete-continuous optimization problem with two types of variables, i.e., binary view selection variables $(\mathbf{x},\mathbf{y})$ as well as continuous power allocation and time allocation variables $(\mathbf{t},\mathbf{p})$. For given $(\mathbf{x},\mathbf{y})$, the optimization with respect to $(\mathbf{t},\mathbf{p})$ is non-convex, as $\sum_{v\in\overline{\mathcal{V}}} t_{\mathbf{h},v}p_{\mathbf{h},v}$ is not convex in $(\mathbf{t}_{\mathbf{h}},\mathbf{p}_{\mathbf{h}})$.

B. Optimal Solution

In this part, we develop an algorithm to obtain an optimal solution of Problem 1. Define $\mathbf{Y} \triangleq \{\mathbf{y} : (4),(5),(6),(7)\}$ and $\mathbf{X}\times\mathbf{Y} \triangleq \{(\mathbf{x},\mathbf{y}) : (3),(8),\mathbf{y}\in\mathbf{Y}\}$. First, by a change of variables, i.e., using $e_{\mathbf{h},v} \triangleq p_{\mathbf{h},v}t_{\mathbf{h},v}$ (representing the transmission energy for view v under $\mathbf{h}$) instead of $p_{\mathbf{h},v}$ for all $\mathbf{h}\in\mathcal{H}^K, v\in\overline{\mathcal{V}}$, and by exploiting structural properties of Problem 1, we obtain an equivalent problem of Problem 1.

Problem 2 (View Selection):

$$\min_{(\mathbf{x},\mathbf{y})\in\mathbf{X}\times\mathbf{Y}} E_{\mathrm{t}}^\star(\mathbf{y}) + \sum_{v\in\overline{\mathcal{V}}\setminus\mathcal{V}} x_v E_b + \beta\sum_{k\in\mathcal{K}}(1-y_{k,r_k})E_{\mathrm{u},k}$$

where $E_{\mathrm{t}}^\star(\mathbf{y})$ is given by the following problem. Let $(\mathbf{x}^\star,\mathbf{y}^\star)$ denote an optimal solution of Problem 2.

Problem 3 (Time and Energy Allocation for Given $\mathbf{y}$): For any given $\mathbf{y}\in\mathbf{Y}$,

$$\begin{aligned} E_{\mathrm{t}}^\star(\mathbf{y}) \triangleq \min_{\mathbf{t},\mathbf{e}} \quad & \mathbb{E}_{\mathbf{H}}\left[\sum_{v\in\overline{\mathcal{V}}} e_{\mathbf{H},v}\right] \\ \text{s.t.} \quad & (9),(10), \\ & e_{\mathbf{h},v}\geq 0, \quad \mathbf{h}\in\mathcal{H}^K,\ v\in\overline{\mathcal{V}}, \qquad (15) \\ & \frac{B}{T}\mathbb{E}_{\mathbf{H}}\left[t_{\mathbf{H},v}\log_2\left(1+\frac{e_{\mathbf{H},v}H_k}{t_{\mathbf{H},v}\sigma^2}\right)\right] \geq y_{k,v}R, \\ & \qquad k\in\mathcal{K},\ v\in\overline{\mathcal{V}}. \qquad (16) \end{aligned}$$

Let $(\mathbf{t}^\star(\mathbf{y}),\mathbf{e}^\star(\mathbf{y}))$ denote an optimal solution of Problem 3, where $\mathbf{t}^\star(\mathbf{y}) \triangleq (t_{\mathbf{h},v}^\star(\mathbf{y}))_{\mathbf{h}\in\mathcal{H}^K,v\in\overline{\mathcal{V}}}$ and $\mathbf{e}^\star(\mathbf{y}) \triangleq (e_{\mathbf{h},v}^\star(\mathbf{y}))_{\mathbf{h}\in\mathcal{H}^K,v\in\overline{\mathcal{V}}}$.

Note that the constraints in (11) and (12) are equivalent to the constraints in (15) and (16), respectively. This formulation (including Problem 2 and Problem 3) separates the two types of variables (i.e., binary variables and continuous variables) and facilitates the optimization. Due to the equivalence between Problem 1 and Problems 2 and 3, we know that $(\mathbf{x}^\star,\mathbf{y}^\star,\mathbf{t}^\star(\mathbf{y}^\star),\mathbf{p}^\star(\mathbf{y}^\star))$ is an optimal solution of Problem 1, where $\mathbf{p}^\star(\mathbf{y}) \triangleq (p_{\mathbf{h},v}^\star(\mathbf{y}))_{\mathbf{h}\in\mathcal{H}^K,v\in\overline{\mathcal{V}}}$ with $p_{\mathbf{h},v}^\star(\mathbf{y}) = e_{\mathbf{h},v}^\star(\mathbf{y})/t_{\mathbf{h},v}^\star(\mathbf{y})$, $\mathbf{h}\in\mathcal{H}^K, v\in\overline{\mathcal{V}}$. Thus, we can obtain an optimal solution of Problem 1 by first solving Problem 3 and then solving Problem 2.

1) Solution of Problem 3: First, we focus on solving Problem 3. Problem 3 is a convex optimization problem and can be solved using standard convex optimization techniques [25].[8] Note that when the sizes of $\mathcal{H}$ and K are large, the numbers of variables and constraints in Problem 3 are huge, leading to high computational complexity. As Problem 3 is convex and strictly feasible, implying that Slater's condition holds, the duality gap is zero. To accelerate the speed for solving Problem 3, we can also adopt partial dual decomposition to enable parallel computation [26]. Specifically, by relaxing the coupling constraints in (16), we obtain a decomposable partial dual problem of Problem 3.

Problem 4 (Partial Dual Problem of Problem 3): For any given $\mathbf{y}\in\mathbf{Y}$,

$$\begin{aligned} D^\star(\mathbf{y}) \triangleq \max_{\boldsymbol{\lambda}} \quad & D(\mathbf{y},\boldsymbol{\lambda}) = \sum_{\mathbf{h}\in\mathcal{H}^K} q_{\mathbf{H}}(\mathbf{h})D_{\mathbf{h}}(\mathbf{y},\boldsymbol{\lambda}) \\ \text{s.t.} \quad & \lambda_{k,v}\geq 0, \quad k\in\mathcal{K},\ v\in\overline{\mathcal{V}}, \end{aligned} \qquad (17)$$

where $\boldsymbol{\lambda} \triangleq (\lambda_{k,v})_{k\in\mathcal{K},v\in\overline{\mathcal{V}}}$. Let $\boldsymbol{\lambda}^\star(\mathbf{y})$ denote an optimal solution of Problem 4. $D_{\mathbf{h}}(\mathbf{y},\boldsymbol{\lambda})$ is given by the following subproblem.

Problem 5 (Subproblem of Problem 4 for $\mathbf{h}\in\mathcal{H}^K$): For any given $\mathbf{y}\in\mathbf{Y}$ and $\boldsymbol{\lambda}\succeq 0$,

$$\begin{aligned} D_{\mathbf{h}}(\mathbf{y},\boldsymbol{\lambda}) \triangleq \min_{\mathbf{t}_{\mathbf{h}},\mathbf{e}_{\mathbf{h}}} \quad & \sum_{v\in\overline{\mathcal{V}}} e_{\mathbf{h},v} \\ & -\sum_{k\in\mathcal{K}}\sum_{v\in\overline{\mathcal{V}}}\lambda_{k,v}\left(\frac{B}{T}t_{\mathbf{h},v}\log_2\left(1+\frac{e_{\mathbf{h},v}h_k}{t_{\mathbf{h},v}\sigma^2}\right)-y_{k,v}R\right) \\ \text{s.t.} \quad & e_{\mathbf{h},v}\geq 0, \quad v\in\overline{\mathcal{V}}, \qquad (18) \\ & t_{\mathbf{h},v}\geq 0, \quad v\in\overline{\mathcal{V}}, \qquad (19) \\ & \sum_{v\in\overline{\mathcal{V}}} t_{\mathbf{h},v}\leq T, \qquad (20) \end{aligned}$$

where $\mathbf{e}_{\mathbf{h}} \triangleq (e_{\mathbf{h},v})_{v\in\overline{\mathcal{V}}}$. Let $(\mathbf{t}_{\mathbf{h}}^\star(\mathbf{y},\boldsymbol{\lambda}),\mathbf{e}_{\mathbf{h}}^\star(\mathbf{y},\boldsymbol{\lambda}))$ denote an optimal solution of Problem 5, where $\mathbf{t}_{\mathbf{h}}^\star(\mathbf{y},\boldsymbol{\lambda}) \triangleq (t_{\mathbf{h},v}^\star(\mathbf{y},\boldsymbol{\lambda}))_{v\in\overline{\mathcal{V}}}$ and $\mathbf{e}_{\mathbf{h}}^\star(\mathbf{y},\boldsymbol{\lambda}) \triangleq (e_{\mathbf{h},v}^\star(\mathbf{y},\boldsymbol{\lambda}))_{v\in\overline{\mathcal{V}}}$.

Define $\mathbf{t}^\star(\mathbf{y},\boldsymbol{\lambda}) \triangleq (\mathbf{t}_{\mathbf{h}}^\star(\mathbf{y},\boldsymbol{\lambda}))_{\mathbf{h}\in\mathcal{H}^K}$ and $\mathbf{e}^\star(\mathbf{y},\boldsymbol{\lambda}) \triangleq (\mathbf{e}_{\mathbf{h}}^\star(\mathbf{y},\boldsymbol{\lambda}))_{\mathbf{h}\in\mathcal{H}^K}$. We have the following result.

[8] In this paper, we assume that the server is aware of the statistics of the random system channel. Thus, the problems considered in this paper are not stochastic optimization problems.

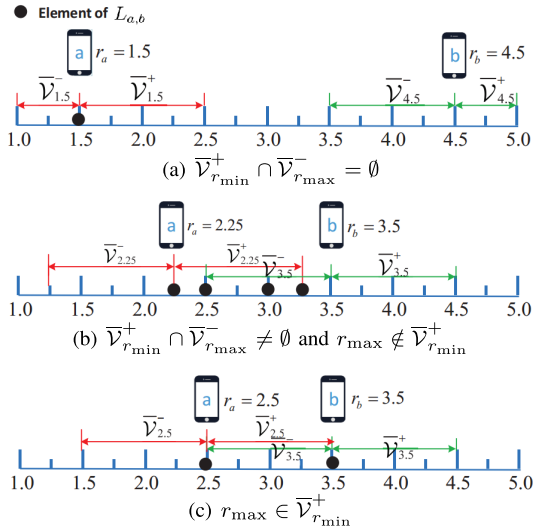

Fig. 2. Illustration of $\mathcal{L}_{a,b}$. $\mathcal{V} = \{1, 2, 3, 4, 5\}$, $\overline{\mathcal{V}} = \{1, 1.25, 1.5, \cdots, 5\}$ and $\Delta_k = 1, k \in \mathcal{K}$.

Lemma 1 (Relationship between Problems 4,5 and Problem 3): For any given $\mathbf{y} \in \mathbf{Y}$, $D^\star(\mathbf{y}) = E_{\mathrm{t}}^\star(\mathbf{y})$, $\mathbf{t}^\star(\mathbf{y}) = \mathbf{t}^\star(\mathbf{y}, \boldsymbol{\lambda}^\star(\mathbf{y}))$ and $\mathbf{e}^\star(\mathbf{y}) = \mathbf{e}^\star(\mathbf{y}, \boldsymbol{\lambda}^\star(\mathbf{y}))$.

Proof: Please refer to Appendix A. ■

By Lemma 1, we can obtain an optimal solution of Problem 3 by solving Problem 4 and Problem 5 for all $\mathbf{h} \in \mathcal{H}^K$. As Problem 5 for all $\mathbf{h} \in \mathcal{H}^K$ can be solved in parallel using standard convex optimization techniques, we can compute $(\mathbf{t}^\star(\mathbf{y}, \boldsymbol{\lambda}), \mathbf{e}^\star(\mathbf{y}, \boldsymbol{\lambda}))$ efficiently. In addition, Problem 4 is convex and can be solved using the subgradient method [27]. In particular, for all $k \in \mathcal{K}, v \in \overline{\mathcal{V}}$, the subgradient method generates a sequence of dual feasible points according to the following update equation:

$$\lambda_{k,v}(n+1) = \max\{\lambda_{k,v}(n) + \eta_{k,v}(n) s_{k,v}(\mathbf{y}, \boldsymbol{\lambda}(n)), 0\}, \tag{21}$$

where $\boldsymbol{\lambda}(n) \triangleq (\lambda_{k,v}(n))_{k \in \mathcal{K}, v \in \overline{\mathcal{V}}}$ and $s_{k,v}(\mathbf{y}, \boldsymbol{\lambda}(n))$ denotes a subgradient of $D(\mathbf{y}, \boldsymbol{\lambda}(n))$ with respect to $\lambda_{k,v}$ given by:

$$s_{k,v}(\mathbf{y}, \boldsymbol{\lambda}(n)) \triangleq y_{k,v} R - \frac{B}{T} \sum_{\mathbf{h} \in \mathcal{H}^K} q_{\mathbf{H}}(\mathbf{h}) t^\star_{\mathbf{h},v}(\mathbf{y}, \boldsymbol{\lambda}(n)) \times \log_2 \left(1 + \frac{e^\star_{\mathbf{h},v}(\mathbf{y}, \boldsymbol{\lambda}(n)) h_k}{t^\star_{\mathbf{h},v}(\mathbf{y}, \boldsymbol{\lambda}(n)) \sigma^2}\right). \tag{22}$$

Here, n denotes the iteration index and $\{\eta_{k,v}(n)\}$ is a step size sequence, satisfying:

$$\eta_{k,v}(n) > 0, \ \sum_{n=0}^{\infty} \eta_{k,v}(n) = \infty, \ \sum_{n=0}^{\infty} \eta^2_{k,v}(n) < \infty, \ \lim_{n \to \infty} \eta_{k,v}(n) = 0.$$

It has been shown in [27] that $\boldsymbol{\lambda}(n) \to \boldsymbol{\lambda}^\star(\mathbf{y})$ as $n \to \infty$, for all initial points $\boldsymbol{\lambda}(0) \succeq 0$. Therefore, we can solve Problem 3 by solving Problem 4 and Problem 5 for all $\mathbf{h} \in \mathcal{H}^K$.

2) Solution of Problem 2: Next, we focus on solving Problem 2, which is a challenging discrete optimization problem. Problem 2 can be solved by exhaustive search over $\mathbf{X} \times \mathbf{Y}$. We would like to reduce the search space by analyzing optimality properties of Problem 2. For any two users $a \in \mathcal{K}$ and $b \in \mathcal{K}$, define $r_{\max} \triangleq \max\{r_a, r_b\}$, $r_{\min} \triangleq \min\{r_a, r_b\}$ and $\mathcal{L}_{a,b}$ is given by (23), as shown at the bottom of the next page. For all user $k \in \mathcal{K}$, define $\mathcal{L}_k \triangleq \bigcup_{i \in \mathcal{K}: i \neq k} \mathcal{L}_{k,i}$. We have the following lemma.

Algorithm 1 Algorithm for Obtaining an Optimal Solution of Problem 1

Output $(\mathbf{x}^\star, \mathbf{y}^\star, \mathbf{t}^\star, \mathbf{p}^\star)$.

1: Set $E^\star = \infty$, $n = 0$, and choose any $\boldsymbol{\lambda}(n) \geq 0$.
2: **for** $(\mathbf{x}, \mathbf{y}) \in \underline{\mathbf{X}} \times \underline{\mathbf{Y}}$ **do**
3: **repeat**
4: For all $\mathbf{h} \in \mathcal{H}^K$, obtain $(\mathbf{t}_{\mathbf{h}}(\mathbf{y}, \boldsymbol{\lambda}(n)), \mathbf{e}_{\mathbf{h}}(\mathbf{y}, \boldsymbol{\lambda}(n)))$ by solving Problem 5 using standard convex optimization techniques.
5: For all $k \in \mathcal{K}$ and $v \in \overline{\mathcal{V}}$, compute $\lambda_{k,v}$ according to (21), where $s_{k,v}(\mathbf{y}, \boldsymbol{\lambda}(n))$ is obtained according to (22).
6: Set $n = n + 1$.
7: **until** convergence criteria is met.
8: For all $\mathbf{h} \in \mathcal{H}^K$, set $\mathbf{t}_{\mathbf{h}}(\mathbf{y}) = \mathbf{t}_{\mathbf{h}}(\mathbf{y}, \boldsymbol{\lambda}(n-1))$ and $\mathbf{e}_{\mathbf{h}}(\mathbf{y}) = \mathbf{e}_{\mathbf{h}}(\mathbf{y}, \boldsymbol{\lambda}(n-1))$.
9: Compute $E(\mathbf{x}, \mathbf{y}) = \sum_{\mathbf{h} \in \mathcal{H}^K} q_{\mathbf{H}}(\mathbf{h}) \mathbf{e}_{\mathbf{h}}(\mathbf{y}) + \sum_{v \in \overline{\mathcal{V}} \setminus \mathcal{V}} x_v E_b + \beta \sum_{k \in \mathcal{K}} (1 - y_{k,r_k}) E_{\mathrm{u},k}$.
10: **if** $E(\mathbf{x}, \mathbf{y}) \leq E^\star$ **then**
11: Obtain $\mathbf{p} = (p_{\mathbf{h},v})_{\mathbf{h} \in \mathcal{H}^K, v \in \overline{\mathcal{V}}}$ where $p_{\mathbf{h},v} = e_{\mathbf{h},v}/t_{\mathbf{h},v}, \mathbf{h} \in \mathcal{H}^K, v \in \overline{\mathcal{V}}$.
12: Set $E^\star = E(\mathbf{x}, \mathbf{y})$ and $(\mathbf{x}^\star, \mathbf{y}^\star, \mathbf{t}^\star, \mathbf{p}^\star) = (\mathbf{x}, \mathbf{y}, \mathbf{t}, \mathbf{p})$.
13: **end if**
14: **end for**

Lemma 2 (Optimality Properties of Problem 2): (i) $x^\star_v = \max_{k \in \mathcal{K}} y^\star_{k,v}$, $v \in \overline{\mathcal{V}}$; (ii) Suppose $\beta E_{\mathrm{u},k} \geq E_{\mathrm{b}}$, $k \in \mathcal{K}$. Then, $y^\star_{k,v} = 0$, $k \in \mathcal{K}$, $v \in \overline{\mathcal{V}} \setminus (\cup_{k \in \mathcal{K}} \mathcal{L}_k)$.

Proof: Please refer to Appendix B. ■

Statement (i) indicates that view v will be transmitted if at least one user utilizes it. $\mathcal{L}_{a,b}$ can be viewed as the set of views that may be utilized by user a when considering the presence of only users a and b, as illustrated in Fig. 2; $\mathcal{L}_k$ can be interpreted as the set of views that may be utilized by user k considering the presence of all users; $\cup_{k \in \mathcal{K}} \mathcal{L}_k$ can be treated as the set of views that may be utilized by at least one user. Thus, Statement (ii) indicates that no views in $\overline{\mathcal{V}} \setminus (\cup_{k \in \mathcal{K}} L_k)$ will be utilized by any user. Lemma 2 characterizes the relationship between $\mathbf{x}^\star$ and $\mathbf{y}^\star$, and determines some zero elements of $\mathbf{y}^\star$. Let $\underline{\mathbf{X}} \times \underline{\mathbf{Y}} \triangleq \{(\mathbf{x}, \mathbf{y}) | \ \mathbf{y} \in \underline{\mathbf{Y}}, x_v = \max_{k \in \mathcal{K}} y_{k,v}, v \in \overline{\mathcal{V}}\}$, where $\underline{\mathbf{Y}} \triangleq \{\mathbf{y} \in \mathbf{Y} | y_{k,v} = 0, v \in \overline{\mathcal{V}} \setminus (\cup_{k \in \mathcal{K}} U_k), k \in \mathcal{K}\}$. Based on Lemma 2, we can reduce the feasible set for (x, y) from $\mathbf{X} \times \mathbf{Y}$ to $\underline{\mathbf{X}} \times \underline{\mathbf{Y}}$ without losing optimality.

3) Algorithm: Based on the results in Section III-B.1 and Section III-B.2, we develop an algorithm to obtain an optimal solution of Problem 1, as summarized in Algorithm 1.

C. Suboptimal Solution

Although the complexity for obtaining an optimal solution of Problem 2 has been reduced based on Lemma 2, the complexity of Algorithm 1 is still unacceptable when K is large. In this part, we propose a low-complexity algorithm to obtain a suboptimal solution of Problem 1.

First, by Lemma 2, we can replace x_v in Problem 1 with $\max_{k\in\mathcal{K}} y_{k,v}$ for all $v \in \overline{\mathcal{V}}$, without loss of optimality. Recalling that $\mathbf{p}$ can be determined by $\mathbf{e}$ and $\mathbf{t}$, we can use $\mathbf{e}$ instead of $\mathbf{p}$. The discrete constraints in (4) can be equivalently transformed to:

$$y_{k,v} \in [0,1], \quad k \in \mathcal{K},\ v \in \overline{\mathcal{V}}, \tag{24}$$

$$y_{k,v}(1-y_{k,v}) \le 0, \quad k \in \mathcal{K},\ v \in \overline{\mathcal{V}}. \tag{25}$$

The reasons are given below. It is clear that (4) implies (24) and (25). By (24), we have $y_{k,v}(1-y_{k,v}) \ge 0,\ k \in \mathcal{K},\ v \in \overline{\mathcal{V}}$. Together with (25), we have $y_{k,v}(1-y_{k,v}) = 0,\ k \in \mathcal{K},\ v \in \overline{\mathcal{V}}$, implying (4). Therefore, (4) is equivalent to (24) and (25). By noting that the constraints in (25) are concave, we can disregard the constraints in (25) and add to the objective function a penalty for violating them [28]. Therefore, we can convert Problem 1 to the following problem.

Problem 6 (Penalized DC Problem of Problem 1):

$$\begin{aligned}\min_{\mathbf{y},\mathbf{t},\mathbf{e}}\ & \mathbb{E}_{\mathbf{H}}\left[\sum_{v\in\overline{\mathcal{V}}} e_{\mathbf{H},v}\right] + E_b \sum_{v\in\overline{\mathcal{V}}\setminus\mathcal{V}} \max_{k\in\mathcal{K}} y_{k,v} \\ & +\beta\sum_{k\in\mathcal{K}}(1-y_{k,r_k})E_{\mathrm{u},k} + \rho P(\mathbf{y}) \\ \text{s.t.}\ & (5),(6),(7),(9),(10),(15),(16),(24),\end{aligned}$$

where the penalty parameter $\rho > 0$ and the penalty function $P(\mathbf{y})$ is given by

$$P(\mathbf{y}) = \sum_{k\in\mathcal{K}}\sum_{v\in\overline{\mathcal{V}}} y_{k,v}(1-y_{k,v}). \tag{26}$$

Note that the objective function of Problem 6 can be viewed as a difference of two convex functions and the feasible set of Problem 6 is convex. Thus, Problem 6 can be viewed as a penalized DC problem of Problem 1. An optimal solution of Problem 6 with zero penalty is also optimal for Problem 1. Now, we solve Problem 6 instead of Problem 1 by using the DC algorithm in [29]. The main idea is to iteratively solve a sequence of convex approximations of Problem 6, each of which is obtained by linearizing the penalty function $P(\mathbf{y})$. Specifically, the convex approximation of Problem 6 at the i-th iteration is given below.

Problem 7 (Convex Approximation of Problem 6 at i-th Iteration):

$$\begin{aligned}(\mathbf{y}^{(i)},\mathbf{t}^{(i)},\mathbf{e}^{(i)}) \triangleq \arg\min_{\mathbf{y},\mathbf{t},\mathbf{e}}\ & \mathbb{E}_{\mathbf{H}}\left[\sum_{v\in\overline{\mathcal{V}}} e_{\mathbf{H},v}\right] \\ & +E_b\sum_{v\in\overline{\mathcal{V}}\setminus\mathcal{V}}\max_{k\in\mathcal{K}} y_{k,v} + \beta\sum_{k\in\mathcal{K}}(1-y_{k,r_k})E_{u,k} \\ & +\rho\hat{P}\left(\mathbf{y};\mathbf{y}^{(i-1)}\right) \\ \text{s.t.}\ & (5),(6),(7),(9),(10),(16),(24),\end{aligned}$$

where

$$\begin{aligned}\hat{P}\left(\mathbf{y};\mathbf{y}^{(i-1)}\right) &\triangleq P\left(\mathbf{y}^{(i-1)}\right) + \nabla P\left(\mathbf{y}^{(i-1)}\right)^T\left(\mathbf{y}-\mathbf{y}^{(i-1)}\right) \\ &= \sum_{k\in\mathcal{K}}\sum_{v\in\overline{\mathcal{V}}}\left(1-2y_{k,v}^{(i-1)}\right)y_{k,v} + \left(y_{k,v}^{(i-1)}\right)^2.\end{aligned}$$

Here, $\mathbf{y}^{(i-1)}$ denotes an optimal solution of Problem 7 at the $(i-1)$-th iteration.

Problem 7 is a convex optimization problem and can be solved using standard convex optimization techniques. Similarly, to improve computation efficiency, we can adopt partial dual decomposition and parallel computation, as in Section III-B. Due to space limitation, we omit the details.

It is known that the sequence $\{(\mathbf{y}^{(i)},\mathbf{t}^{(i)},\mathbf{e}^{(i)})\}$ generated by the DC algorithm is convergent, and its limit point is a stationary point of Problem 6. We can run the DC algorithm multiple times, each with a random initial feasible point of Problem 6. Then, we select the stationary point with the minimum average weighted sum energy among those with zero penalty, denoted by $\{(\mathbf{y}^\dagger,\mathbf{t}^\dagger,\mathbf{e}^\dagger)\}$. Due to the equivalence between Problems 1 and 6, we know that for sufficiently large ρ, we can obtain a feasbile solution of Problem 1 based on $(\mathbf{y}^\dagger,\mathbf{t}^\dagger,\mathbf{e}^\dagger)$ as follows. Based on $\mathbf{y}^\dagger$, we obtain $\mathbf{x}^\dagger \triangleq (x_v^\dagger)_{v\in\overline{\mathcal{V}}}$ according to Lemma 2 (i). Based on $\mathbf{t}^\dagger$ and $\mathbf{e}^\dagger$, we then compute $\mathbf{p}^\dagger \triangleq (p_{\mathbf{h},v}^\dagger)_{v\in\overline{\mathcal{V}},\mathbf{h}\in\mathcal{H}^K}$ using $p_{\mathbf{h},v}^\dagger = e_{\mathbf{h},v}^\dagger/t_{\mathbf{h},v}^\dagger$. $(\mathbf{x}^\dagger,\mathbf{y}^\dagger,\mathbf{t}^\dagger,\mathbf{p}^\dagger)$ can serve as a suboptimal solution of Problem 1. The details are summarized in Algorithm 2.[9]

IV. Total Utility Maximization

In this section, we consider the total utility maximization under the energy consumption constraints for the server and each user. We first formulate the optimization problem. Then, we develop a low-complexity algorithm to obtain a suboptimal solution using DC programming.

A. Problem Formulation

First, we impose the energy consumption constraints for the server and each user:

$$\mathbb{E}_{\mathbf{H}}\left[\sum_{v\in\overline{\mathcal{V}}} t_{\mathbf{H},v}p_{\mathbf{H},v}\right] + \sum_{v\in\overline{\mathcal{V}}\setminus\mathcal{V}} x_v E_b \le \bar{E}_b, \tag{27}$$

$$(1-y_{k,r_k})E_{\mathrm{u},k} \le \bar{E}_{\mathrm{u},k}, \quad k\in\mathcal{K}, \tag{28}$$

where $\bar{E}_b$ and $\bar{E}_{\mathrm{u},k}$ represent the energy consumption limits (for each time slot) at the server and user k, respectively. We would like to maximize the total utility by optimizing the view selection, transmission time and power allocation, and quality selection under the energy consumption constraints.

[9]Note that in Algorithm 2, $\mathbb{E}_{\mathbf{H}}\left[\sum_{v\in\overline{\mathcal{V}}} e_{\mathbf{H},v}^{(i)}\right] = \sum_{\mathbf{h}\in\mathcal{H}^K} q_{\mathbf{H}}(\mathbf{h})\sum_{v\in\overline{\mathcal{V}}} e_{\mathbf{H},v}^{(i)}$ can be computed as $q_{\mathbf{H}}(\mathbf{h}), \mathbf{h}\in\mathcal{H}^K$ are known.

$$\mathcal{L}_{a,b} \triangleq \begin{cases}\{r_a\}, & \overline{\mathcal{V}}^+_{r_{\min}} \cap \overline{\mathcal{V}}^-_{r_{\max}} = \emptyset, \\ \{r_a, r_{\max}-\Delta, r_{\min}+\Delta\} \cup (\overline{\mathcal{V}}^+_{r_{\min}} \cap \overline{\mathcal{V}}^-_{r_{\max}} \cap \mathcal{V}), & \overline{\mathcal{V}}^+_{r_{\min}} \cap \overline{\mathcal{V}}^-_{r_{\max}} \ne \emptyset \text{ and } r_{\max} \notin \overline{\mathcal{V}}^+_{r_{\min}}, \\ \{r_a, r_b, r_{\max}-\Delta, r_{\min}+\Delta\}, & r_{\max} \in \overline{\mathcal{V}}^+_{r_{\min}}\end{cases} \tag{23}$$

Algorithm 2 Algorithm for Obtaining a Suboptimal Solution of Problem 1

Input $c \geq 1$

Output $(\mathbf{x}^\dagger, \mathbf{y}^\dagger, \mathbf{t}^\dagger, \mathbf{p}^\dagger)$

1: $E = +\infty$.
2: **while** $c > 0$ **do**
3: Find a random feasible point of Problem 6 as the initial point $(\mathbf{y}^{(0)}, \mathbf{t}^{(0)}, \mathbf{e}^{(0)})$, choose a sufficiently large ρ, and set $i = 0$.
4: **repeat**
5: Set $i = i + 1$.
6: Obtain $(\mathbf{y}^{(i)}, \mathbf{t}^{(i)}, \mathbf{e}^{(i)})$ of Problem 7 using standard convex optimization techniques or partial dual decomposition and parallel computation (similar to Steps 3-7 in Algorithm 1).
7: **until** convergence criteria is met.
8: **if** $P(\mathbf{y}^{(i)}) = 0$ **then**
9: Set $c = c - 1$.
10: **if** $\mathbb{E}_{\mathbf{H}}\left[\sum_{v\in\overline{\mathcal{V}}} e^{(i)}_{\mathbf{H},v}\right] + E_b \sum_{v\in\overline{\mathcal{V}}\setminus\mathcal{V}} \max_{k\in\mathcal{K}} y^{(i)}_{k,v} + \beta\sum_{k\in\mathcal{K}}(1 - y^{(i)}_{k,r_k})E_{\mathrm{u},k} < E$ **then**
11: Set $E = \mathbb{E}_{\mathbf{H}}\left[\sum_{v\in\overline{\mathcal{V}}} e^{(i)}_{\mathbf{H},v}\right] + E_b \sum_{v\in\overline{\mathcal{V}}\setminus\mathcal{V}} \max_{k\in\mathcal{K}} y^{(i)}_{k,v} + \beta\sum_{k\in\mathcal{K}}(1 - y^{(i)}_{k,r_k})E_{\mathrm{u},k}$, $\mathbf{x}^\dagger = (x^\dagger_v)_{v\in\overline{\mathcal{V}}}$, $\mathbf{y}^\dagger = \mathbf{y}^{(i)}$, $\mathbf{t}^\dagger = \mathbf{t}^{(i)}$ and $\mathbf{p}^\dagger = (p^\dagger_{\mathbf{h},v})_{\mathbf{h}\in\mathcal{H}^K, v\in\overline{\mathcal{V}}}$, where $x^\dagger_v = \max y^{(i)}_{k,v}, v \in \overline{\mathcal{V}}$ and $p^\dagger_{\mathbf{h},v} = e^{(i)}_{\mathbf{h},v}/t^{(i)}_{\mathbf{h},v}, \mathbf{h} \in \mathcal{H}^K, v \in \overline{\mathcal{V}}$.
12: **end if**
13: **end if**
14: **end while**

Specifically, for given $\bar{E}_b$ and $\bar{E}_{\mathrm{u},k}, k \in \mathcal{K}$, we have the following optimization problem.

Problem 8 (Total Utility Maximization):

$$\max_{\mathbf{x},\mathbf{y},\mathbf{t},\mathbf{p},\boldsymbol{\Delta}} \quad U(\boldsymbol{\Delta}) \\ \text{s.t.} \quad (1), (3) - (12), (27), (28).$$

Let $(\mathbf{x}^\star, \mathbf{y}^\star, \mathbf{t}^\star, \mathbf{p}^\star, \boldsymbol{\Delta}^\star)$ denote an optimal solution of Problem 8 with slight abuse of notation, where $\boldsymbol{\Delta}^\star \triangleq (\Delta^\star_k)_{k\in\mathcal{K}}$.

Problem 8 is a challenging mixed discrete-continuous optimization problem with two types of variables, i.e., discrete view selection variables and quality selection variables $(\mathbf{x}, \mathbf{y}, \boldsymbol{\Delta})$ as well as continuous power and time allocation variables $(\mathbf{t}, \mathbf{p})$. Problem 8 is even more challenging than Problem 1, as it has extra discrete variables $\boldsymbol{\Delta}$ and the constraint functions of $\boldsymbol{\Delta}$ in (5)-(7) are not tractable.

B. Suboptimal Solution

In this part, we propose a low-complexity algorithm to obtain a suboptimal solution of Problem 8 using equivalent transformations and DC programming. First, we transform Problem 8 to an equivalent penalized DC Problem which can be solved using DC programming. Specifically, we relax the discrete constraints in (1) to:

$$1 \leq \Delta_k \leq V - 1, \quad k \in \mathcal{K}. \tag{29}$$

Then, we transform the constraints in (5)-(7) to the following constraints:

$$y_{k,r_k} + \sum_{v>r_k, v\in\overline{\mathcal{V}}} y_{k,v} = 1, \quad k \in \mathcal{K}, \tag{30}$$

$$v - r_k - \Delta_k \leq c(1 - y_{k,v}), \quad v \in \overline{\mathcal{V}},\ k \in \mathcal{K}, \tag{31}$$

$$y_{k,r_k} + \sum_{v<r_k, v\in\overline{\mathcal{V}}} y_{k,v} = 1, \quad k \in \mathcal{K}, \tag{32}$$

$$r_k - v - \Delta_k \leq c(1 - y_{k,v}), \quad v \in \overline{\mathcal{V}},\ k \in \mathcal{K}, \tag{33}$$

where $c > V - 2$ is a positive constant. Next, as for solving Problem 1, we eliminate $\mathbf{x}$, use $\mathbf{e}$ instead of $\mathbf{p}$, convert the discrete constraints in (4) to the continuous constraints in (24) and (25), and disregard (25) by adding to the objective function a penalty for violating (25). Therefore, we can convert Problem 8 to the following problem.

Problem 9 (Penalized DC Problem of Problem 8):

$$\max_{\mathbf{y},\mathbf{t},\mathbf{e},\boldsymbol{\Delta}} \quad U(\boldsymbol{\Delta}) - \rho P(\mathbf{y}) \\ \text{s.t.} \quad (3), (9), (10), (15), (16), (24), (28) - (33) \\ \mathbb{E}_{\mathbf{H}}\left[\sum_{v\in\overline{\mathcal{V}}} e_{\mathbf{H},v}\right] + E_b \sum_{v\in\overline{\mathcal{V}}\setminus\mathcal{V}} \max_{k\in\mathcal{K}} y_{k,v} \leq \bar{E}_b, \tag{34}$$

where $P(\mathbf{y})$ is given by (26). Let $(\mathbf{y}^*, \mathbf{t}^*, \mathbf{e}^*, \boldsymbol{\Delta}^*)$ denote an optimal solution of Problem 9.

The following result shows the relationship between Problem 8 and Problem 9.

Theorem 1 (Relationship between Problem 8 and Problem 9): If $P(\mathbf{y}^*) = 0$, for all $c > V - 2$, $\mathbf{y}^\star = \mathbf{y}^*$, $\mathbf{t}^\star = \mathbf{t}^*$, $\mathbf{p}^\star = \mathbf{p}^*$ and $\boldsymbol{\Delta}^\star = \boldsymbol{\Delta}^*$, where $\mathbf{p}^* = (p^*_{\mathbf{h},v})_{\mathbf{h}\in\mathcal{H}^K, v\in\overline{\mathcal{V}}}$ with $p^*_{\mathbf{h},v} = e^*_{\mathbf{h},v}/t^*_{\mathbf{h},v}, \mathbf{h} \in \mathcal{H}^K, v \in \overline{\mathcal{V}}$.

Proof: Please refer to Appendix C. ∎

We can obtain a stationary point of Problem 9, denoted by $(\mathbf{y}^\dagger, \mathbf{t}^\dagger, \mathbf{p}^\dagger, \boldsymbol{\Delta}^\dagger)$ with $P(\mathbf{y}^\dagger) = 0$, using DC programming. By Theorem 1, we know that $(\mathbf{y}^\dagger, \mathbf{t}^\dagger, \mathbf{p}^\dagger, \boldsymbol{\Delta}^\dagger)$ is a feasible solution of Problem 8. Similarly, based on $\mathbf{y}^\dagger$, we can obtain $\mathbf{x}^\dagger \triangleq (x^\dagger_v)_{v\in\overline{\mathcal{V}}}$ with $x^\dagger_v = \max_{k\in\mathcal{K}} y_{k,v}, v \in \overline{\mathcal{V}}$. Based on $\mathbf{t}^\dagger$ and $\mathbf{e}^\dagger$, we then compute $\mathbf{p}^\dagger \triangleq (p^\dagger_{\mathbf{h},v})_{v\in\overline{\mathcal{V}},\mathbf{h}\in\mathcal{H}^K}$ where $p^\dagger_{\mathbf{h},v} = e^\dagger_{\mathbf{h},v}/t^\dagger_{\mathbf{h},v}, \mathbf{h} \in \mathcal{H}^K, v \in \overline{\mathcal{V}}$. $(\mathbf{x}^\dagger, \mathbf{y}^\dagger, \mathbf{p}^\dagger, \mathbf{t}^\dagger, \boldsymbol{\Delta}^\dagger)$ serves as a suboptimal solution of Problem 8. The details are summarized in Algorithm 3.

V. Numerical Results

In the simulation, we set $\beta = 2$, $R = 18.59$ Mbit/s,[10] $E_b = 10^{-3}$ Joule, $E_{\mathrm{u},k} = 10^{-3}$ Joule, $k \in \mathcal{K}$ [24], $\mathcal{V} = \{1, 2, 3, 4, 5\}$, $B = 10$ MHz,[11] $T = 100$ ms, $U_k(\Delta_k) = V - \Delta_k, k \in \mathcal{K}$ and $\sigma^2 = Bk_BT_0$, where $k_B = 1.38\times10^{-23}$ Joule/Kelvin is the Boltzmann constant and $T_0 = 300$ Kelvin is the temperature. For ease of simulation, we consider two channel states, i.e., a good channel state and a bad channel state, and set $\mathcal{H} = \{0.5d, 1.5d\}$, $\Pr[H_k = 0.5d] = 0.5$ and $\Pr[H_k = 1.5d] = 0.5$ for all $k \in \mathcal{K}$, where $d = 10^{-6}$

[10]We use MVV sequence *Kendo* as the video source [30] and use HEVC in FFmpeg to encode the video with quantization parameter 15, frame rate 30 frame/s and resolution 1024×768.

[11]We consider a multi-carrier TDMA with 10 channels, each with bandwidth 1 MHz.

Algorithm 3 Algorithm for Obtaining a Suboptimal Solution of Problem 8

Input $c \geq 1$

Output $(\mathbf{x}^\dagger, \mathbf{y}^\dagger, \mathbf{t}^\dagger, \mathbf{p}^\dagger, \mathbf{\Delta}^\dagger)$

1: Set $U = 0$.
2: **while** $c > 0$ **do**
3: Find a random feasible point of Problem 8 as the initial point $(\mathbf{y}^{(0)}, \mathbf{t}^{(0)}, \mathbf{e}^{(0)}, \mathbf{\Delta}^{(0)})$, choose a sufficiently large ρ and $c > V - 2$, and set $i = 0$.
4: Obtain $(\mathbf{y}^{(i)}, \mathbf{t}^{(i)}, \mathbf{e}^{(i)}, \mathbf{\Delta}^{(i)})$ based on DC programming (similar to Steps 4-7 in Algorithm 2).
5: **if** $P(\mathbf{y}^{(i)}) = 0$ **then**
6: Set $c = c - 1$.
7: **if** $U(\mathbf{\Delta}^{(i)}) > U$ **then**
8: Set $U = U(\mathbf{\Delta}^{(i)})$, $\mathbf{x}^\dagger = (x_v^\dagger)_{v \in \overline{\mathcal{V}}}$, $\mathbf{y}^\dagger = \mathbf{y}^{(i)}$, $\mathbf{t}^\dagger = \mathbf{t}^{(i)}$, $\mathbf{p}^\dagger = (p^\dagger_{\mathbf{h},v})_{\mathbf{h} \in \mathcal{H}^K, v \in \overline{\mathcal{V}}}$ and $\mathbf{\Delta}^\dagger = \mathbf{\Delta}^{(i)}$, where $x_v^\dagger = \max_{k \in \mathcal{K}} y_{k,v}^{(i)}, v \in \overline{\mathcal{V}}$ and $p^\dagger_{\mathbf{h},v} = e^{(i)}_{\mathbf{h},v}/t^{(i)}_{\mathbf{h},v}, \mathbf{h} \in \mathcal{H}^K, v \in \overline{\mathcal{V}}$.
9: **end if**
10: **end if**
11: **end while**

reflects the path loss. In addition, we assume that the K users randomly request views in an i.i.d. manner. Specifically, for all $k \in \mathcal{K}$, r_k falls in two regions, i.e., $\mathcal{V}_1 \triangleq \{2, 2+\frac{1}{Q}, \cdots, 4\}$ and $\mathcal{V}_2 \triangleq \{1, 1+\frac{1}{Q}, \cdots, 1+\frac{Q-1}{Q}\} \cup \{4+\frac{1}{Q}, \cdots, 5\}$, according to Zipf distribution with Zipf exponent γ,[12] i.e., $\Pr[r_k \in \mathcal{V}_1] = \frac{1^{-\gamma}}{\sum_{v \in \{1,2\}} v^{-\gamma}} \triangleq P_1$ and $\Pr[r_k \in \mathcal{V}_2] = \frac{2^{-\gamma}}{\sum_{v \in \{1,2\}} v^{-\gamma}} \triangleq P_2$. Note that a smaller γ indicates a longer tail. Furthermore, for all $k \in \mathcal{K}$, a view in $\mathcal{V}_1$ or $\mathcal{V}_2$ is requested according to the uniform distribution, i.e., $\Pr[r_k = v] = \frac{P_1}{2Q+1}, v \in \mathcal{V}_1$ and $\Pr[r_k = v] = \frac{P_2}{2Q}, v \in \mathcal{V}_2$. We randomly generate 100 view requests for all users, and evaluate the average performance over these realizations.

For comparison, we consider two commonly used view selection mechanisms, based on which we shall construct optimization-based baseline schemes to minimize the weighted sum energy consumption and maximize the total utility, respectively. In one view slection mechanism, the view requested by each user is transmitted [18]. In our setup, this requires view synthesis at the server but does not consider view synthesis at each user, and hence is referred to as the synthesis-server mechanism here. More specifically, for all $k \in \mathcal{K}$ and $v \in \overline{\mathcal{V}}$, $y_{k,v} = 1$ if $v = r_k$, and $y_{k,v} = 0$ otherwise; for all $v \in \overline{\mathcal{V}}$, $x_v = \max_{k \in \mathcal{K}} y_{k,v}$. In the other view selection mechanism, no synthesized views will be transmitted. In our setup, this requires view synthesis at each user but does not consider view synthesis at the server [20], and hence is referred to as the synthesis-user mechanism here. More specifically, for all $k \in \mathcal{K}$, $y_{k,v} = 0$ if $v \notin \mathcal{V} \cap (\{r_k\} \cup \overline{\mathcal{V}}^-_{k,r_k} \cup \overline{\mathcal{V}}^+_{k,r_k})$. We use Matlab and CVX toolbox to implement the proposed solutions and baseline schemes which are all optimization-based designs.

[12]Note that Zipf distribution is widely used to model content popularity in Internet and wireless networks. In addition, the proposed solutions and their properties are valid for arbitrary distributions of view requests.

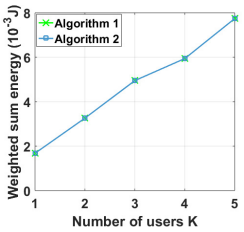

(a) Weighted sum energy versus K.

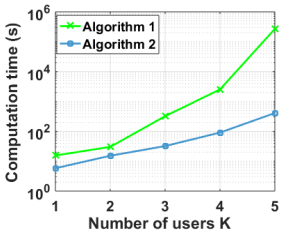

(b) Computation time versus K.

Fig. 3. Comparison between the optimal solution and suboptimal solution at $\Delta_k = 1$, $k \in \mathcal{K}$, $Q = 5$ and $\gamma = 1$.

A. Weighted Sum Energy Minimization

In this part, we compare the weighted sum energy consumptions of the proposed optimal and suboptimal solutions with those of two baseline schemes at $\Delta_k = 1, k \in \mathcal{K}$. First, we compare the proposed optimal solution (obtained using Algorithm 1) with the proposed suboptimal solution of Problem 1 (obtained using Algorithm 2) at small[13] numbers of users. Fig. 3 illustrates the weighted sum energy consumption and computation time (reflecting computational complexity) versus the number of users, respectively. From Fig. 3 (a), we can see that the weighted sum energy consumption of the suboptimal solution is the same as that of the optimal solution when K is small (under our setup). From Fig. 3 (b), we can see that the computation time of the suboptimal solution grows with the number of users at a much smaller rate than that of the optimal solution. This numerical example demonstrates the applicability and efficiency of the suboptimal solution.

Next, we compare the proposed suboptimal solution of Problem 1 with two baseline schemes, i.e., the synthesis-server-energy scheme and the synthesis-user-energy scheme. The two schemes adopt the synthesis-server mechanism and the synthesis-user mechanism, respectively. In addition, the synthesis-server-energy scheme adopts the optimal power and time allocation obtained by solving Problem 3 with $(\mathbf{x}, \mathbf{y})$ chosen according to the synthesis-server mechanism using Steps 3-13 of Algorithm 1; the synthesis-user-energy scheme adopts the power and time allocation and view selection obtained by solving Problem 1 with extra constraints on $\mathbf{y}$ which are imposed according to the synthesis-user mechanism using Algorithm 2. Note that leveraging on our proposed transmission mechanism, both baseline schemes can utilize natural multicast opportunities; the synthesis-server-energy scheme does not create view synthesis-enabled multicast opportunities, but it can guarantee to transmit no more than K views; the synthesis-user-energy scheme can create view synthesis-enabled multicast opportunities, but it may cause extra transmissions (i.e., may transmit more than K views).

Fig. 4 illustrates the weighted sum energy consumptions versus the number of users K, Zipf exponent γ and view spacing $1/Q$. From Fig. 4 (a), we can see that the weighted sum energy consumption of each scheme increases with K, as the traffic load increases with K. From Fig. 4 (b) and Fig. 4 (c), we can see that the weighted sum energy consumption of each

[13]Note that the computational complexity of Algorithm 1 is not acceptable when K is large.

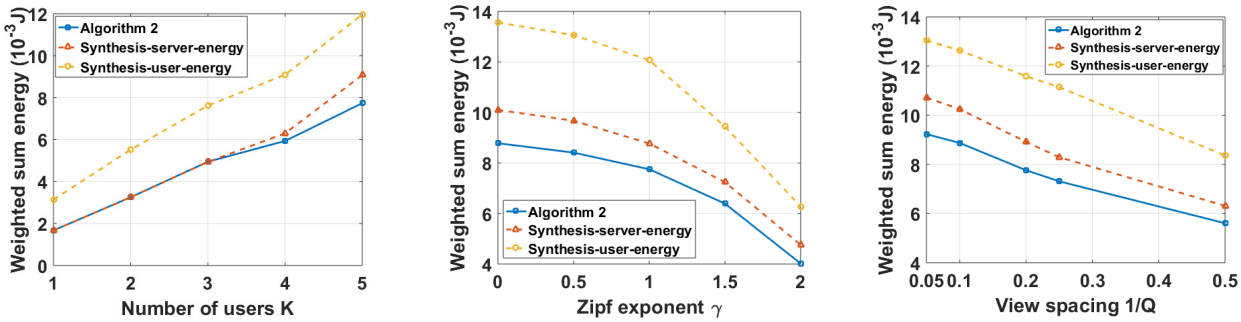

(a) Weighted sum energy versus K at $\Delta_k = 1$, $k \in \mathcal{K}$, $Q = 5$ and $\gamma = 1$. (b) Weighted sum energy versus γ at $\Delta_k = 1$, $k \in \mathcal{K}$, $Q = 5$ and $K = 5$. (c) Weighted sum energy versus $1/Q$ at $\Delta_k = 1$, $k \in \mathcal{K}$, $\gamma = 1$ and $K = 5$.

Fig. 4. Comparison between the suboptimal solution and two baseline schemes.

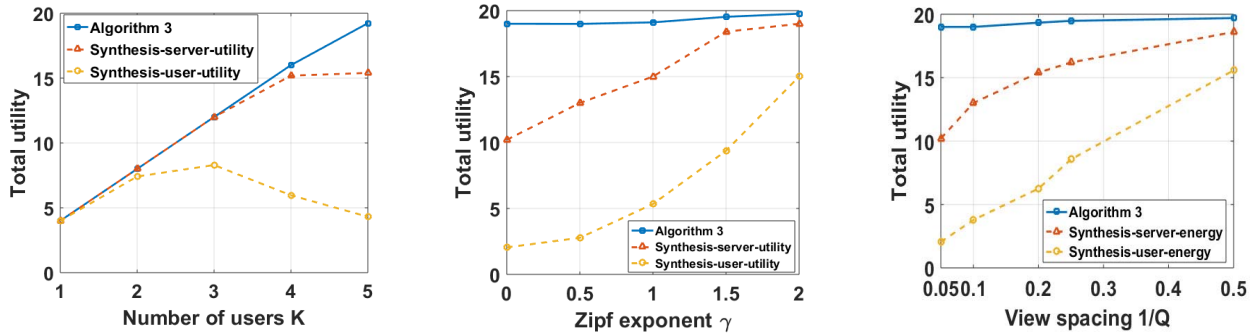

(a) Total utility versus K at $\gamma = 1$, $Q = 5$ and $\bar{E}_b = 10 \times 10^{-3}$ Joule and $\bar{E}_{\mathrm{u},k} = 10^{-3}$ Joule, $k \in \mathcal{K}$. (b) Total utility versus γ at $K = 5$, $Q = 5$ and $\bar{E}_b = 10 \times 10^{-3}$ Joule and $\bar{E}_{\mathrm{u},k} = 10^{-3}$ Joule, $k \in \mathcal{K}$. (c) Total utility versus $1/Q$ at $\gamma = 1$, $K = 5$ and $\bar{E}_b = 10 \times 10^{-3}$ Joule and $\bar{E}_{\mathrm{u},k} = 10^{-3}$ Joule, $k \in \mathcal{K}$.

Fig. 5. Comparison between the suboptimal solution and two baseline schemes.

scheme decreases with γ and with $1/Q$. This is because a larger γ or a lager $1/Q$ indicates that view requests from the users are more concentrated, leading to more natural multicast opportunities. From Fig. 4, we can see that the synthesis-server-energy scheme outperforms the synthesis-user-energy scheme in most cases, demonstrating that creating view synthesis-enabled multicast opportunities in a naive manner usually causes extra transmissions and yields a higher weighted sum energy consumption; the proposed suboptimal solution outperforms the two baseline schemes, revealing the importance of the optimization of view synthesis-enabled multicast opportunities in reducing energy consumption. Note that the gains of the proposed suboptimal solution over the baseline schemes are large at large K, small γ or small $1/Q$, as more view synthesis-enabled multicast opportunities can be created in these regions.

B. Total Utility Maximization

In this part, we compare the total utilities of the proposed suboptimal solution of Problem 8 (obtained using Algorithm 3) and two baselines, i.e., the synthesis-server-utility scheme and the synthesis-user-utility scheme, at $\bar{E}_b = 10 \times 10^{-3}$ Joule and $\bar{E}_{\mathrm{u},k} = 10^{-3}$ Joule, $k \in \mathcal{K}$.[14] The two baseline schemes adopt the synthesis-server mechanism and the synthesis-user mechanism, respectively. In addition, the synthesis-server-utility scheme chooses $\Delta_k = \min\{\Delta_k | (1), (5), (6), (7)\}$, $k \in \mathcal{K}$ with $(\mathbf{x}, \mathbf{y})$ in (5), (6) and (7) chosen according to the synthesis-server mechanism, and achieves total utility $U(\mathbf{\Delta})$ if Problem 8 with its choice for $(\mathbf{x}, \mathbf{y}, \mathbf{\Delta})$ is feasible; the synthesis-user-utility scheme achieves the total utility that is obtained by solving Problem 8 with extra constraints on $\mathbf{y}$ which are set according to the synthesis-user mechanism using Algorithm 3. Note that the synthesis-server-utility scheme and the synthesis-user-utility scheme share the same properties on natural and view synthesis-enabled multicast opportunities as the synthesis-server-energy scheme and the synthesis-user-energy scheme, respectively. For a realization of $r_k, k \in \mathcal{K}$, if the problem for each scheme is infeasible, we set the total utility to be 0, for ease of comparison.

Fig. 5 illustrates the total utility versus the number of users K, Zipf exponent γ and view spacing $1/Q$. From Fig. 5 (a), we can see that the total utility of each scheme increases with K when K is small, as there is enough energy for serving more users; the total utilities of two baseline schemes no longer increase with K when K becomes large, as $\bar{E}_b$ and $\bar{E}_{\mathrm{u},k}, k \in \mathcal{K}$ are not large enough and the optimization of the two baseline schemes are more likely to be infeasible under random user requests. From Fig. 5 (b) and Fig. 5 (c), we can see that the total utility of each scheme increases with γ and with $1/Q$, as natural multicast opportunities increase with γ and with $1/Q$. Finally, from Fig. 5, we see that the suboptimal solution outperforms the two baseline schemes, also revealing the importance of the optimization of view synthesis-enabled multicast opportunities in improving the total utility. Similarly, we can see that the gains of the proposed

[14]Note that for each scheme, the constraints in (28) are always satisfied under the choices for $E_{\mathrm{u},k}, k \in \mathcal{K}$ and $\bar{E}_{\mathrm{u},k}, k \in \mathcal{K}$.

suboptimal solution over the baseline schemes are large at large K, small γ or small $1/Q$, as more view synthesis-enabled multicast opportunities can be created in these regions.

VI. Conclusion

In this paper, we considered optimal MVV transmission in a multiuser wireless network by exploiting both natural multicast opportunities and view synthesis-enabled multicast opportunities. First, we established a mathematical model to specify view synthesis at the server and each user and characterize its impact on multicast opportunities. To the best of our knowledge, this is the first mathematical model that enables the optimization of view synthesis-enabled multicast opportunities. Then, we considered the minimization of the weighted sum energy consumption for view transmission and synthesis for given quality requirements of all users. We also considered the maximization of the total utility under the energy consumption constraints at the server and each user. These two optimization problems are challenging mixed discrete-continuous optimization problems. We proposed an algorithm to obtain an optimal solution of the first problem with reduced computational complexity, by exploiting optimality properties. In addition, for each problem, we proposed a low-complexity algorithm to obtain a suboptimal solution, using DC programming. Finally, using numerical results, we showed the advantage of the proposed solutions, and demonstrated the importance of view synthesis-enabled multicast opportunities in MVV transmission.

Appendix A: Proof of Lemma 1

First, we relax the coupling constraints in (16) and obtain the following partial Lagrange function $L(\mathbf{y},\mathbf{t},\mathbf{e},\boldsymbol{\lambda})$, given by (35), as shown at the bottom of this page, where $\lambda_{k,v}, k \in \mathcal{K}, v \in \overline{\mathcal{V}}$ denote the Lagrange multipliers with respect to the constraints in (16) and $L_{\mathbf{h}}(\mathbf{y},\mathbf{t}_{\mathbf{h}},\mathbf{e}_{\mathbf{h}},\boldsymbol{\lambda}) \triangleq \sum_{v\in\overline{\mathcal{V}}} e_{\mathbf{h},v} - \sum_{k\in\mathcal{K}}\sum_{v\in\overline{\mathcal{V}}}\lambda_{k,v}\left(\frac{B}{T}t_{\mathbf{h},v}\log_2\left(1+\frac{e_{\mathbf{h},v}h_k}{t_{\mathbf{h},v}\sigma^2}\right) - y_{k,v}R\right)$. Next, for any given $\mathbf{y}\in\mathbf{Y}$, we obtain the corresponding partial dual function of Problem 3:

$$D(\mathbf{y},\boldsymbol{\lambda}) \triangleq \min_{\mathbf{t},\mathbf{e}} \quad L(\mathbf{y},\mathbf{t},\mathbf{e},\boldsymbol{\lambda}) \quad \text{s.t.} \quad (9),(10),(15),$$

where $L(\mathbf{y},\mathbf{t},\mathbf{e},\boldsymbol{\lambda})$ is given by (35). As the objective function and constraints are separable, this problem can be equivalently decomposed into Problem 5, one for each $\mathbf{h}\in\mathcal{H}^K$. As the duality gap for Problem 3 is zero, we can show Lemma 1.

Appendix B: Proof of Lemma 2

A. Proof of Statement (i)

We prove Statement (i) by contradiction. Suppose there exists $v_0 \in \overline{\mathcal{V}}$ such that $x^\star_{v_0} \neq \max_{k\in\mathcal{K}} y^\star_{k,v_0}$. By (8), this implies $x^\star_{v_0} > \max_{k\in\mathcal{K}} y^\star_{k,v_0}$. By (3) and (4), we know $x^\star_{v_0}=1$ and $y^\star_{k,v_0}=0$, $k\in\mathcal{K}$. Construct $\mathbf{x}^\dagger \triangleq (x^\dagger_v)_{v\in\overline{\mathcal{V}}}$ with $x^\dagger_{v_0}=0$ and $x^\dagger_v = x^\star_v, v\neq v_0, v\in\overline{\mathcal{V}}$. It is clear that $\mathbf{x}^\dagger$ and $\mathbf{y}^\star$ satisfy (3) and (8). In addition, the objective function of Problem 1, i.e., $\mathbb{E}_{\mathbf{H}}\left[E(\mathbf{x},\mathbf{y},\mathbf{t}_{\mathbf{H}},\mathbf{p}_{\mathbf{H}})\right]$ increases with x_v, $v\in\overline{\mathcal{V}}$, and the constraints in (5), (6), (7), (9), (10), (11), (12) do not rely on $\mathbf{x}$. Therefore, $(\mathbf{x}^\dagger,\mathbf{y}^\star,\mathbf{t}^\star,\mathbf{p}^\star)$ is a feasible solution with a smaller objective value than the optimal solution $(\mathbf{x}^\star,\mathbf{y}^\star,\mathbf{t}^\star,\mathbf{p}^\star)$. Therefore, by contradiction, we can prove Statement (i).

B. Proof of Statement (ii)

We prove Statement (ii) by contradiction. Suppose that there exist $k_0\in\mathcal{K}$ and $v_0\in\overline{\mathcal{V}}\setminus(\cup_{k\in\mathcal{K}}L_k)$ such that $y^\star_{k_0,v_0}=1$. In the following, we consider three cases, i.e., $v_0\notin\overline{\mathcal{V}}^-_{r_{k_0}}\cup\overline{\mathcal{V}}^+_{r_{k_0}}$, $v_0\in\overline{\mathcal{V}}^+_{r_{k_0}}$ and $v_0\in\overline{\mathcal{V}}^-_{r_{k_0}}$. In each case, we construct a feasible solution which achieves a smaller objective value under the assumption. Thus, by contradiction, we can show Statement (ii).

1) $v_0 \notin \overline{\mathcal{V}}^-_{r_{k_0}}\cup\overline{\mathcal{V}}^+_{r_{k_0}}$: First, we construct $\mathbf{y}^\dagger \triangleq (y^\dagger_{k,v})_{k\in\mathcal{K},v\in\overline{\mathcal{V}}}$ with $y^\dagger_{k_0,v_0}=0$ and $y^\dagger_{k,v}=y^\star_{k,v}$, $(k,v)\neq(k_0,v_0), (k,v)\in\mathcal{K}\times\overline{\mathcal{V}}$, and $\mathbf{x}^\dagger\triangleq(x^\dagger_v)_{v\in\overline{\mathcal{V}}}$ with $x^\dagger_{v_0}=0$ and $x^\dagger_v=x^\star_v, v\neq v_0, v\in\overline{\mathcal{V}}$. It is easy to show that $(\mathbf{x}^\dagger,\mathbf{y}^\dagger,\mathbf{t}^\star,\mathbf{p}^\star)$ is a feasible solution with a smaller objective value than $(\mathbf{x}^\star,\mathbf{y}^\star,\mathbf{t}^\star,\mathbf{p}^\star)$.

2) $v_0\in\overline{\mathcal{V}}^+_{r_{k_0}}$: First, define $\mathcal{K}_{v_0}\triangleq\{k\in\mathcal{K}\,|y_{k,v_0}=1\}$, $v_1\triangleq\max_{k\in\mathcal{K}_{v_0}} f_{v_0}(r_k)$, and $\mathcal{M}_{v_0}\triangleq\{k\in\mathcal{K}_{v_0}|r_k=v_1\}$ where

$$f_{v_0}(r_k)\triangleq\begin{cases} r_k & r_k<v_0\\ r_k-\Delta & r_k>v_0\end{cases}.$$

By (5) and $y^\star_{k,v_0}=1$, we know $y^\star_{k,v_1}=0$ for all $k\in\mathcal{K}_{v_0}$. Construct $\mathbf{y}^\dagger\triangleq(y^\dagger_{k,v})_{k\in\mathcal{K},v\in\overline{\mathcal{V}}}$ with $y^\dagger_{k,v_1}=1, y^\dagger_{k,v_0}=0$, $y^\dagger_{k,v}=y^\star_{k,v}, v\in\overline{\mathcal{V}}\setminus\{v_0,v_1\}$, $k\in\mathcal{K}_{v_0}$ and $y^\dagger_{k,v}=y^\star_{k,v}, v\in\overline{\mathcal{V}}, k\in\mathcal{K}\setminus\mathcal{K}_{v_0}$; construct $\mathbf{x}^\dagger\triangleq(x^\dagger_v)_{v\in\overline{\mathcal{V}}}$ with $x^\dagger_v=\max_{k\in\mathcal{K}}y^\dagger_{k,v}, v\in\overline{\mathcal{V}}$; construct $\mathbf{t}^\dagger\triangleq(t^\dagger_{\mathbf{h},v})_{\mathbf{h}\in\mathcal{H}^K,v\in\overline{\mathcal{V}}}$ with $t^\dagger_{\mathbf{h},v_0}=0, t^\dagger_{\mathbf{h},v_1}=\max\{t^\star_{\mathbf{h},v_0},t^\star_{\mathbf{h},v_1}\}$ and $t^\dagger_{\mathbf{h},v}=t^\star_{\mathbf{h},v}, v\in\overline{\mathcal{V}}\setminus\{v_0,v_1\}$, $\mathbf{h}\in\mathcal{H}^K$; construct $\mathbf{p}^\dagger\triangleq(p_{\mathbf{h},v})_{\mathbf{h}\in\mathcal{H}^K,v\in\overline{\mathcal{V}}}$ with $p^\dagger_{\mathbf{h},v_0}=0, p^\dagger_{\mathbf{h},v_1}=\max\{t^\star_{\mathbf{h},v_0}p^\star_{\mathbf{h},v_0}, t^\star_{\mathbf{h},v_1}p^\star_{\mathbf{h},v_1}\}/t^\dagger_{\mathbf{h},v_1}$ and $p^\dagger_{\mathbf{h},v}=p^\star_{\mathbf{h},v}, v\in\overline{\mathcal{V}}\setminus\{v_0,v_1\}$ for all $\mathbf{h}\in\mathcal{H}^K$.

Next, we show that $(\mathbf{x}^\dagger,\mathbf{y}^\dagger,\mathbf{t}^\dagger,\mathbf{p}^\dagger)$ is a feasible solution of Problem 1. It is clear that $(\mathbf{x}^\dagger,\mathbf{y}^\dagger,\mathbf{t}^\dagger,\mathbf{p}^\dagger)$ satisfies the

$$\begin{aligned} L(\mathbf{y},\mathbf{t},\mathbf{e},\boldsymbol{\lambda}) &\triangleq \sum_{\mathbf{h}\in\mathcal{H}^K} q_{\mathbf{H}}(\mathbf{h})\sum_{v\in\overline{\mathcal{V}}} e_{\mathbf{h},v} - \sum_{k\in\mathcal{K}}\sum_{v\in\overline{\mathcal{V}}}\lambda_{k,v}\left(\frac{B}{T}\sum_{\mathbf{h}\in\mathcal{H}^K} q_{\mathbf{H}}(\mathbf{h})t_{\mathbf{h},v}\log_2\left(1+\frac{e_{\mathbf{h},v}h_k}{t_{\mathbf{h},v}\sigma^2}\right) - y_{k,v}R\right)\\ &= \sum_{\mathbf{h}\in\mathcal{H}^K} q_{\mathbf{H}}(\mathbf{h})L_{\mathbf{h}}(\mathbf{y},\mathbf{t}_{\mathbf{h}},\mathbf{e}_{\mathbf{h}},\boldsymbol{\lambda}) \end{aligned} \tag{35}$$

constraints in (3), (4), (5), (6), (7), (8), (9) and (11). Then, we show that $(\mathbf{y}^\dagger, \mathbf{t}^\dagger, \mathbf{p}^\dagger)$ satisfies the constraints in (10) and (12). Since $\sum_{v\in\overline{\mathcal{V}}} t^\dagger_{\mathbf{h},v} \overset{(a)}{\leq} \sum_{v\in\overline{\mathcal{V}}} t^\star_{\mathbf{h},v} \leq T,\ \mathbf{h}\in\mathcal{H}^K$, where (a) is due to $t^\dagger_{\mathbf{h},v_0}=0, t^\dagger_{\mathbf{h},v_1}=\max\{t^\star_{\mathbf{h},v_0}, t^\star_{\mathbf{h},v_1}\}, \mathbf{h}\in\mathcal{H}^K$ and $t^\dagger_{\mathbf{h},v}=t^\star_{\mathbf{h},v}, \mathbf{h}\in\mathcal{H}^K, v\in\overline{\mathcal{V}}\setminus\{v_0,v_1\}$, we can show that $\mathbf{t}^\dagger$ satisfies the constraints in (10). By the construction of $(\mathbf{x}^\dagger, \mathbf{y}^\dagger, \mathbf{t}^\dagger, \mathbf{p}^\dagger)$, we know:

$$\frac{B}{T}\mathbb{E}_{\mathbf{H}}\left[t^\dagger_{\mathbf{H},v}\log_2\left(1+\frac{p^\dagger_{\mathbf{H},v}H_k}{\sigma^2}\right)\right] \geq y^\dagger_{k,v}R, \quad k\in\mathcal{K},\ v\in\overline{\mathcal{V}}\setminus\{v_1\}. \tag{36}$$

In addition, we have

$$\begin{aligned}
&\frac{B}{T}\mathbb{E}_{\mathbf{H}}\left[t^\dagger_{\mathbf{H},v_1}\log_2\left(1+\frac{p^\dagger_{\mathbf{H},v_1}H_k}{\sigma^2}\right)\right]\\
&=\frac{B}{T}\mathbb{E}_{\mathbf{H}}\left[t^\dagger_{\mathbf{H},v_1}\log_2\left(1+\frac{t^\dagger_{\mathbf{H},v_1}p^\dagger_{\mathbf{H},v_1}H_k}{t^\dagger_{\mathbf{H},v_1}\sigma^2}\right)\right]\\
&\overset{(b)}{\geq}\frac{B}{T}\mathbb{E}_{\mathbf{H}}\left[t^\star_{\mathbf{H},v}\log_2\left(1+\frac{t^\star_{\mathbf{H},v}p^\star_{\mathbf{H},v}H_k}{t^\star_{\mathbf{H},v}\sigma^2}\right)\right], \quad k\in\mathcal{K},\ v\in\{v_0,v_1\}\\
&\Rightarrow\frac{B}{T}\mathbb{E}_{\mathbf{H}}\left[t^\dagger_{\mathbf{H},v_1}\log_2\left(1+\frac{p^\dagger_{\mathbf{H},v_1}H_k}{\sigma^2}\right)\right]\\
&\geq\frac{B}{T}\max_{v\in\{v_0,v_1\}}\left\{\mathbb{E}_{\mathbf{H}}\left[t^\star_{\mathbf{H},v}\log_2\left(1+\frac{t^\star_{\mathbf{H},v}p^\star_{\mathbf{H},v}H_k}{t^\star_{\mathbf{H},v}\sigma^2}\right)\right]\right\}\\
&\overset{(c)}{\geq} R\max_{v\in\{v_0,v_1\}} y^\star_{k,v}\overset{(d)}{=}y^\dagger_{k,v_1}R, \quad k\in\mathcal{K},
\end{aligned}\tag{37}$$

where (b) is due to that $x\log_2(1+y/x)$ is monotonically increasing with respect to x and y, respectively, $t^\dagger_{\mathbf{h},v_1}p^\dagger_{\mathbf{h},v_1}\geq t^\star_{\mathbf{h},v}p^\star_{\mathbf{h},v}$, and $t^\dagger_{\mathbf{h},v_1}=t^\star_{\mathbf{h},v}, \mathbf{h}\in\mathcal{H}^K, v\in\{v_0,v_1\}$, (c) is due to the constraints in (12) for $(\mathbf{y}^\star, \mathbf{t}^\star, \mathbf{p}^\star)$, and (d) is due to $y^\dagger_{k,v_1}=y^\star_{k,v_0}=1,\ k\in\mathcal{K}_{v_0}$ and $y^\dagger_{k,v_1}=y^\star_{k,v_1}, y^\star_{k,v_0}=0,\ k\in\mathcal{K}\setminus\mathcal{K}_{v_0}$. By (36) and (37), we know that $(\mathbf{y}^\dagger, \mathbf{t}^\dagger, \mathbf{p}^\dagger)$ satisfies the constraints in (12). Thus, $(\mathbf{x}^\dagger, \mathbf{y}^\dagger, \mathbf{t}^\dagger, \mathbf{p}^\dagger)$ is a feasible solution of Problem 1.

Finally, we prove $E^\star \geq E^\dagger \triangleq \mathbb{E}_{\mathbf{H}}\left[E(\mathbf{x}^\dagger, \mathbf{y}^\dagger, \mathbf{t}^\dagger_{\mathbf{H}}, \mathbf{p}^\dagger_{\mathbf{H}})\right]$. By the construction of $(\mathbf{x}^\dagger, \mathbf{y}^\dagger, \mathbf{t}^\dagger, \mathbf{p}^\dagger)$, we have (38), which is shown at the bottom of this page, where (e) is due to $x+y-\max\{x,y\}\geq 0$ for all $x,y\geq 0$ and $x^\star_{v_1}-x^\dagger_{v_1}\geq -1$. It remains to show $(x^\star_{v_0}-1)E_b+\beta\sum_{k\in\mathcal{M}_{v_0}}E_{\mathrm{u},k}\geq 0$. We prove this by considering two cases.

- *Case 1:* $v_1\in\{r_k \mid k\in\mathcal{K}\}$. In this case, we have $(x^\star_{v_0}-1)E_b+\beta\sum_{k\in\mathcal{M}_{v_0}}E_{\mathrm{u},k}\geq -E_b+\beta\sum_{k\in\mathcal{M}_{v_0}}E_{\mathrm{u},k}\overset{(f)}{\geq}0$ where (f) is due to $\mathcal{M}_{v_0}\neq\emptyset$ (as $v_1\in\{r_k\mid k\in\mathcal{K}\}$) and $-E_b+\beta E_{u,k}\geq 0$ for all $k\in\mathcal{K}$.
- *Case 2:* $v_1\notin\{r_k \mid k\in\mathcal{K}\}$. First, by $v_1=\max_{k\in\mathcal{K}_{v_0}} f_{v_0}(r_k)$, we know that there exists $k'\in\mathcal{K}_{v_0}$ such that $r_{k'}>v_0$. Thus we have $\overline{\mathcal{V}}^+_{r_{k_0}}\cap\overline{\mathcal{V}}^-_{r_{k'}}\cap\mathcal{V}\subseteq L_{k_0,k'}$ and $v_0\in\overline{\mathcal{V}}\setminus(\cup_{k\in\mathcal{K}}L_k)$, implying that $v_0\notin\overline{\mathcal{V}}^+_{r_{k_0}}\cap\overline{\mathcal{V}}^-_{r_{k'}}\cap\mathcal{V}$. In addition, by noting that $y^\star_{k,v_0}=1, k\in\mathcal{K}_{v_0}$, we have $x^\star_{v_0}=\max_{k\in\mathcal{K}}y_{k,v_0}=1$. Thus, we have $(x^\star_{v_0}-1)E_b+\beta\sum_{k\in\mathcal{M}_{v_0}}E_{\mathrm{u},k}\overset{(g)}{\geq}0$, where (g) is due to $\mathcal{M}_{v_0}=\emptyset$ (as $v_1\notin\{r_k\mid k\in\mathcal{K}\}$) and $x^\star_{v_0}=1$.

Therefore, $(\mathbf{x}^\dagger, \mathbf{y}^\dagger, \mathbf{t}^\star, \mathbf{p}^\star)$ is a feasible solution with a smaller objective value than $(\mathbf{x}^\star, \mathbf{y}^\star, \mathbf{t}^\star, \mathbf{p}^\star)$.

3) $v_0\in\overline{\mathcal{V}}^-_{r_{k_0}}$*:* The argument for $v_0\in\overline{\mathcal{V}}^-_{r_{k_0}}$ is similar to that for $v_0\in\overline{\mathcal{V}}^+_{r_{k_0}}$ and is omitted due to page limitation.

APPENDIX C: PROOF OF THEOREM 1

First, we show that Problem 8 and its continuous relaxation have the same optimal solution. By relaxing the discrete constraints in (1) into (29), we have:

Problem 10 (Continuous Relaxation of Problem 8):

$$\max_{\mathbf{x},\mathbf{y},\mathbf{t},\mathbf{p},\boldsymbol{\Delta}}\ U(\boldsymbol{\Delta}) \quad \text{s.t.}\ \ (3)-(12),(27),(28),(29).$$

Let $(\mathbf{x}^\dagger, \mathbf{y}^\dagger, \mathbf{p}^\dagger, \mathbf{t}^\dagger, \boldsymbol{\Delta}^\dagger)$ denote an optimal solution of Problem 10.

Note that the only difference between Problem 8 and Problem 10 is that $\boldsymbol{\Delta}$ in Problem 8 satisfy (1) and $\boldsymbol{\Delta}$ in Problem 10 satisfy (29). As the fact that $\boldsymbol{\Delta}$ satisfy (1) implies that $\boldsymbol{\Delta}$ satisfy (29), the optimal value of Problem 8 is no greater than the optimal value of Problem 10. Thus, to show that an optimal solution of Problem 10 is also an optimal solution of Problem 8, it remains to show that the optimal solution of Problem 10 satisfies (1). We prove this by contradiction. Suppose $\boldsymbol{\Delta}^\dagger$ does not satisfy (1). Based on $\boldsymbol{\Delta}^\dagger$, we construct $\underline{\boldsymbol{\Delta}}^\dagger\triangleq(\underline{\Delta}^\dagger_k)_{k\in\mathcal{K}}$, where $\underline{\Delta}^\dagger_k=\max\{x\mid x\leq\Delta^\dagger_k,(1)\}$. It is clear that for all $k\in\mathcal{K}$, $\epsilon_k\triangleq\Delta^\dagger_k-\underline{\Delta}^\dagger_k\in[0,1/Q)$. As $U(\boldsymbol{\Delta})$ is a strictly decreasing function of $\boldsymbol{\Delta}$ and $\Delta^\dagger_k\geq\underline{\Delta}^\dagger_k, k\in\mathcal{K}$, we have $U(\underline{\boldsymbol{\Delta}}^\dagger)\geq U(\boldsymbol{\Delta}^\dagger)$. It remains to show that $(\mathbf{x}^\dagger, \mathbf{y}^\dagger, \mathbf{p}^\dagger, \mathbf{t}^\dagger, \underline{\boldsymbol{\Delta}}^\dagger)$ is a feasible solution of Problem 10. Note that only the constraints in (5), (6) and (7) involve $\boldsymbol{\Delta}$.

$$\begin{aligned}
&E^\star-E^\dagger\\
&=\mathbb{E}_{\mathbf{H}}\left[t^\star_{\mathbf{H},v_0}p^\star_{\mathbf{H},v_0}+t^\star_{\mathbf{H},v_1}p^\star_{\mathbf{H},v_1}-t^\dagger_{\mathbf{H},v_0}p^\dagger_{\mathbf{H},v_0}-t^\dagger_{\mathbf{H},v_1}p^\dagger_{\mathbf{H},v_1}\right]+(x^\star_{v_0}+x^\star_{v_1}-x^\dagger_{v_0}-x^\dagger_{v_1})E_b+\beta\sum_{k\in\mathcal{K}}\left(y^\dagger_{k,r_k}-y^\star_{k,r_k}\right)E_{\mathrm{u},k}\\
&=\mathbb{E}_{\mathbf{H}}\left[t^\star_{\mathbf{H},v_0}p^\star_{\mathbf{H},v_0}+t^\star_{\mathbf{H},v_1}p^\star_{\mathbf{H},v_1}-\max\{t^\star_{\mathbf{H},v_0}p^\star_{\mathbf{H},v_0},t^\star_{\mathbf{H},v_1}p^\star_{\mathbf{H},v_1}\}-0\right]+(x^\star_{v_0}+x^\star_{v_1}-0-x^\dagger_{v_1})E_b+\beta\sum_{k\in\mathcal{M}_{v_0}}E_{\mathrm{u},k}\\
&\overset{(e)}{\geq}(x^\star_{v_0}-1)E_b+\beta\sum_{k\in\mathcal{M}_{v_0}}E_{\mathrm{u},k}
\end{aligned}\tag{38}$$

Thus, it is sufficient to show for all $k \in \mathcal{K}$: (i) $\{x \in \overline{\mathcal{V}} : r_k < x \leq r_k + \Delta_k^\dagger\} = \{x \in \overline{\mathcal{V}} : r_k < x \leq r_k + \underline{\Delta}_k^\dagger\}$, (ii) $\{x \in \overline{\mathcal{V}} : r_k - \Delta_k^\dagger \leq x < r_k\} = \{x \in \overline{\mathcal{V}} : r_k - \underline{\Delta}_k^\dagger \leq x < r_k\}$, and (iii) $\{x \in \overline{\mathcal{V}} : x < r_k - \Delta_k^\dagger\} \cup \{x \in \overline{\mathcal{V}} : r_k + \Delta_k^\dagger < x\} = \{x \in \overline{\mathcal{V}} : x < r_k - \underline{\Delta}_k^\dagger\} \cup \{x \in \overline{\mathcal{V}} : r_k + \underline{\Delta}_k^\dagger < x\}$. We prove Case (i) as follows:

$$\begin{aligned}
&\{x \in \overline{\mathcal{V}} : r_k < x \leq r_k + \Delta_k^\dagger\} \\
&\quad = \{x \in \overline{\mathcal{V}} : r_k < x \leq r_k + \underline{\Delta}_k^\dagger + \epsilon_k\} \\
&\quad = \{x \in \overline{\mathcal{V}} : r_k < x \leq r_k + \underline{\Delta}_k^\dagger\} \\
&\qquad\qquad \cup \{x \in \overline{\mathcal{V}} : r_k + \underline{\Delta}_k^\dagger < x \leq r_k + \underline{\Delta}_k^\dagger + \epsilon_k\} \\
&\quad \overset{(a)}{=} \{x \in \overline{\mathcal{V}} : r_k < x \leq r_k + \underline{\Delta}_k^\dagger\} \cup \emptyset \\
&\quad = \{x \in \overline{\mathcal{V}} : r_k < x \leq r_k + \underline{\Delta}_k^\dagger\}, \qquad (39)
\end{aligned}$$

where (a) is due to that $r_k + \underline{\Delta}_k^\dagger \in \overline{\mathcal{V}}$, $\epsilon_k < 1/Q$ and the view spacing is $1/Q$. Case (ii) and Case (iii) can be proved in a similar way to Case (i), and hence are omitted due to page limitation. Thus, we have shown that $(\mathbf{x}^\dagger, \mathbf{y}^\dagger, \mathbf{p}^\dagger, \mathbf{t}^\dagger, \underline{\mathbf{\Delta}}^\dagger)$ is a feasible of Problem 10 with a larger objective value than $(\mathbf{x}^\dagger, \mathbf{y}^\dagger, \mathbf{p}^\dagger, \mathbf{t}^\dagger, \mathbf{\Delta}^\dagger)$, which contradicts the optimality of $(\mathbf{x}^\dagger, \mathbf{y}^\dagger, \mathbf{p}^\dagger, \mathbf{t}^\dagger, \mathbf{\Delta}^\dagger)$. Thus, we know that Problem 8 and Problem 10 have the same optimal solution.

Next, we show that Problem 10 and the following problem have the same optimal solution.

Problem 11 (Transformed Problem of Problem 8):

$$\begin{aligned}
&\max_{\mathbf{x},\mathbf{y},\mathbf{t},\mathbf{p},\mathbf{\Delta}} \quad U(\mathbf{\Delta}) \\
&\text{s.t.} \quad (3), (4), (8), (9), (10), (11), (12), (27) - (33).
\end{aligned}$$

By comparing the constraints of Problem 10 and those of Problem 11, it is sufficient to show that the constraints in (4) and (30)-(33) are equivalent to the constraints in (4)-(7), i.e., $\mathbf{Y} = \mathbf{Y}'$, where $\mathbf{Y} = \{\mathbf{y} : (4), (5), (6), (7)\}$ and $\mathbf{Y}' \triangleq \{\mathbf{y} : (4), (30), (31), (32), (33)\}$. By (4) and (7), we have $y_{k,v} = 0, k \in \mathcal{K}, v \in \{x \in \overline{\mathcal{V}} : x < r_k - \Delta_k\} \cup \{x \in \overline{\mathcal{V}} : r_k + \Delta_k < x\}$. Thus, given that (4) and (7) hold, (5) and (6) are equivalent to (30) and (32). Then, to show $\mathbf{Y} = \mathbf{Y}'$, it is sufficient to show $\{\mathbf{y}_k : (4), (7)\} = \{\mathbf{y}_k : (4), (31), (33)\}$, for all $k \in \mathcal{K}$, where $\mathbf{y}_k \triangleq (y_{k,v})_{v \in \overline{\mathcal{V}}}$. We prove this by considering three cases for $k \in \mathcal{K}$: (i) $v \in \overline{\mathcal{V}}_1 \triangleq \{x \in \overline{\mathcal{V}} : r_k - \Delta_k \leq v \leq r_k + \Delta_k\}$, (ii) $v \in \overline{\mathcal{V}}_2 \triangleq \{x \in \overline{\mathcal{V}} : x > r_k + \Delta_k\}$, and (iii) $v \in \overline{\mathcal{V}}_3 \triangleq \{x \in \overline{\mathcal{V}} : x < r_k - \Delta_k\}$.

- *Case (i):* In this case, as (7) for k is void, $\{(y_{k,v})_{v \in \overline{\mathcal{V}}_1} : (4), (7)\} = \{(y_{k,v})_{v \in \overline{\mathcal{V}}_1} : (4)\}$. In addition, in this case, it is obvious that $v - r_k - \Delta_k \leq 0$ and $r_k - v - \Delta_k \leq 0$. By (4) and $c > 0$, we have $c(1 - y_{k,v}) \geq 0 \geq v - r_k - \Delta_k$ and $c(1 - y_{k,v}) \geq 0 \geq r_k - v - \Delta_k$. Thus, in this case, (31) and (33) hold for k, implying $\{(y_{k,v})_{v \in \overline{\mathcal{V}}_1} : (4), (31), (33)\} = \{(y_{k,v})_{v \in \overline{\mathcal{V}}_1} : (4)\}$. Therefore, we can show $\{(y_{k,v})_{v \in \overline{\mathcal{V}}_1} : (4), (7)\} = \{(y_{k,v})_{v \in \overline{\mathcal{V}}_1} : (4), (31), (33)\}$.
- *Case (ii):* In this case, $\{(y_{k,v})_{v \in \overline{\mathcal{V}}_2} : (4), (7)\} = \{(y_{k,v})_{v \in \overline{\mathcal{V}}_2} : y_{k,v} = 0\}$. In this case, as $r_k - v - \Delta_k < r_k - v + \Delta_k < 0$, (33) always holds for k. Thus, it remains to show $\{(y_{k,v})_{v \in \overline{\mathcal{V}}_2} : y_{k,v} = 0\} = \{(y_{k,v})_{v \in \overline{\mathcal{V}}_2} : (4), (31)\}$. First, we show that $\{(y_{k,v})_{v \in \overline{\mathcal{V}}_2} : (4), (31)\}$ implies $\{(y_{k,v})_{v \in \overline{\mathcal{V}}_2} : y_{k,v} = 0\}$. By $r_k + \Delta_k \geq 2$, $c > V - 2$ and $V \geq v$, we have $c > v - r_k - \Delta_k > 0$, which implies:

$$0 < \frac{v - r_k - \Delta_k}{c} < 1. \qquad (40)$$

In addition, by (31) and $c > V - 2 \geq 0$, we have:

$$y_{k,v} \leq 1 - \frac{v - r_k - \Delta_k}{c}. \qquad (41)$$

By (4), (40) and (41), we have $y_{k,v} = 0, v \in \overline{\mathcal{V}}_2$. That is, $\{(y_{k,v})_{v \in \overline{\mathcal{V}}_2} : (4), (31)\}$ implies $\{(y_{k,v})_{v \in \overline{\mathcal{V}}_2} : y_{k,v} = 0\}$. Next, it is obvious that $\{(y_{k,v})_{v \in \overline{\mathcal{V}}_2} : y_{k,v} = 0\}$ implies $\{(y_{k,v})_{v \in \overline{\mathcal{V}}_2} : (4), (31)\}$. Therefore, we can show $\{(y_{k,v})_{v \in \overline{\mathcal{V}}_2} : (4), (7)\} = \{(y_{k,v})_{v \in \overline{\mathcal{V}}_2} : (4), (31), (33)\}$.

- *Case (iii):* In this case, $\{(y_{k,v})_{v \in \overline{\mathcal{V}}_3} : (4), (7)\} = \{(y_{k,v})_{v \in \overline{\mathcal{V}}_3} : y_{k,v} = 0\}$. In this case, as $v - r_k - \Delta_k < v - r_k + \Delta_k < 0$, (31) always holds for k. Thus, it remains to show $\{(y_{k,v})_{v \in \overline{\mathcal{V}}_3} : y_{k,v} = 0\} = \{(y_{k,v})_{v \in \overline{\mathcal{V}}_3} : (4), (33)\}$. First, we show that $\{(y_{k,v})_{v \in \overline{\mathcal{V}}_3} : (4), (33)\}$ implies $\{(y_{k,v})_{v \in \overline{\mathcal{V}}_3} : y_{k,v} = 0\}$. By $v + \Delta_k \geq 2$, $c > V - 2$ and $V \geq r_k$, we have $c > r_k - v - \Delta_k > 0$, which implies:

$$0 < \frac{r_k - v - \Delta_k}{c} < 1. \qquad (42)$$

By (33) and $c > V - 2 \geq 0$, we have:

$$y_{k,v} \leq 1 - \frac{r_k - v - \Delta_k}{c}. \qquad (43)$$

By (4), (42) and (43), we have $y_{k,v} = 0, v \in \overline{\mathcal{V}}_3$. That is, $\{(y_{k,v})_{v \in \overline{\mathcal{V}}_3} : (4), (33)\}$ implies $\{(y_{k,v})_{v \in \overline{\mathcal{V}}_3} : y_{k,v} = 0\}$. Next, it is obvious that $\{(y_{k,v})_{v \in \overline{\mathcal{V}}_3} : y_{k,v} = 0\}$ implies $\{(y_{k,v})_{v \in \overline{\mathcal{V}}_3} : (4), (33)\}$. Therefore, we can show $\{(y_{k,v})_{v \in \overline{\mathcal{V}}_3} : (4), (7)\} = \{(y_{k,v})_{v \in \overline{\mathcal{V}}_3} : (4), (31), (33)\}$.

Therefore, we can show that Problem 10 and Problem 11 have the same optimal solution.

Finally, Problem 11 is a DC problem and Problem 9 can be viewed as its penalized DC problem. It can be easily shown that an optimal solution of Problem 9 with zero penalty is also an optimal solution of Problem 11.

Therefore, we complete the proof of Theorem 1.

REFERENCES

[1] W. Xu, Y. Wei, Y. Cui, and Z. Liu, "Energy-efficient multi-view video transmission with view synthesis-enabled multicast," in *Proc. IEEE Global Telecommun. Conf.*, Dec. 2018, pp. 1–7.

[2] C. Fehn, "Depth-image-based rendering (DIBR), compression, and transmission for a new approach on 3D-TV," *Proc. SPIE*, vol. 5291, pp. 93–105, May 2004.

[3] A. Smolic *et al.*, "3D video and free viewpoint video—Technologies, applications and MPEG standards," in *Proc. IEEE Int. Conf. Multimedia Expo*, Jul. 2006, pp. 2161–2164.

[4] A. Smolic and P. Kauff, "Interactive 3-D video representation and coding technologies," *Proc. IEEE*, vol. 93, no. 1, pp. 98–110, Jan. 2005.

[5] Digi-Capital Blog, "Augmented virtual reality revenue forecast revised to hit 120 billion by 2020," Accessed: Mar. 10, 2019. [Online]. Available: https://www.digi-capital.com/news/2016/01/augmentedvirtual-reality-revenue-forecast-revised-to-hit-120-billion-by-2020/

[6] A. Vetro, T. Wiegand, and G. J. Sullivan, "Overview of the stereo and multiview video coding extensions of the H.264/MPEG-4 AVC standard," *Proc. IEEE*, vol. 99, no. 4, pp. 626–642, Apr. 2011.

[7] P. Merkle, A. Smolic, K. Müller, and T. Wiegand, "Multi-view video plus depth representation and coding," in *Proc. IEEE Int. Conf. Image Process.*, Oct. 2006, pp. I-201–I-204.

[8] T. Wiegand, G. J. Sullivan, G. Bjøntegaard, and A. Luthra, "Overview of the H.264/AVC video coding standard," *IEEE Trans. Circuits Syst. Video Technol.*, vol. 13, no. 7, pp. 560–576, Jul. 2003.

[9] T. Fujihashi, Z. Pan, and T. Watanabe, "UMSM: A traffic reduction method on multi-view video streaming for multiple users," *IEEE Trans. Multimedia*, vol. 16, no. 1, pp. 228–241, Jan. 2014.

[10] A. D. Abreu, P. Frossard, and F. Pereira, "Optimizing multiview video plus depth prediction structures for interactive multiview video streaming," *IEEE J. Sel. Topics Signal Process.*, vol. 9, no. 3, pp. 487–500, Apr. 2015.

[11] A. De Abreu, P. Frossard, and F. Pereira, "Optimized MVC prediction structures for interactive multiview video streaming," *IEEE Signal Process. Lett.*, vol. 20, no. 6, pp. 603–606, Jun. 2013.

[12] P. Merkle, A. Smolic, K. Müller, and T. Wiegand, "Efficient prediction structures for multiview video coding," *IEEE Trans. Circuits Syst. Video Technol.*, vol. 17, no. 11, pp. 1461–1473, Nov. 2007.

[13] Z. Liu, G. Cheung, and Y. Ji, "Optimizing distributed source coding for interactive multiview video streaming over lossy networks," *IEEE Trans. Circuits Syst. Video Technol.*, vol. 23, no. 10, pp. 1781–1794, Oct. 2013.

[14] L. Toni and P. Frossard, "Optimal representations for adaptive streaming in interactive multiview video systems," *IEEE Trans. Multimedia*, vol. 19, no. 12, pp. 2775–2787, Dec. 2017.

[15] L. Toni, G. Cheung, and P. Frossard, "In-network view synthesis for interactive multiview video systems," *IEEE Trans. Multimedia*, vol. 18, no. 5, pp. 852–864, May 2016.

[16] J. Chakareski, V. Velisavljević, and V. Stanković, "User-action-driven view and rate scalable multiview video coding," *IEEE Trans. Image Process.*, vol. 22, no. 9, pp. 3473–3484, Sep. 2013.

[17] X. Zhang, L. Toni, P. Frossard, Y. Zhao, and C. Lin, "Adaptive streaming in interactive multiview video systems," *IEEE Trans. Circuits Syst. Video Technol.*, vol. 29, no. 4, pp. 1130–1144, Apr. 2019.

[18] Q. Zhao, Y. Mao, S. Leng, and G. Min, "Qos-aware energy-efficient multicast for multi-view video with fractional frequency reuse," in *Proc. 10th Int. Conf. Commun. Netw. China (ChinaCom)*, Aug. 2015, pp. 567–572.

[19] Q. Zhao, Y. Mao, S. Leng, and Y. Jiang, "QoS-aware energy-efficient multicast for multi-view video in indoor small cell networks," in *Proc. Global Commun. Conf. (GLOBECOM)*, Dec. 2014, pp. 4478–4483.

[20] X. Zhang, Y. Zhao, T. Tillo, and C. Lin, "A packetization strategy for interactive multiview video streaming over lossy networks," *Signal Process.*, vol. 145, pp. 285–294, Apr. 2018.

[21] J. Wu, Q. Zhao, N. Yang, and J. Duan, "Augmented reality multi-view video scheduling under vehicle-pedestrian situations," in *Proc. Int. Conf. Connected Vehicles Expo (ICCVE)*, Oct. 2015, pp. 163–168.

[22] L. Toni, N. Thomos, and P. Frossard, "Interactive free viewpoint video streaming using prioritized network coding," in *Proc. IEEE 15th Int. Workshop Multimedia Signal Process. (MMSP)*, Sep. 2013, pp. 446–451.

[23] C. Guo, Y. Cui, and Z. Liu, "Optimal multicast of tiled 360 VR video," *IEEE Wireless Commun. Lett.*, vol. 8, no. 1, pp. 145–148, Feb. 2019.

[24] J. Llorca, K. Guan, G. Atkinson, and D. C. Kilper, "Energy efficient delivery of immersive video centric services," in *Proc. IEEE INFOCOM*, Mar. 2012, pp. 1656–1664.

[25] S. Boyd and L. Vandenberghe, *Convex Optimization*. Cambridge, U.K.: Cambridge Univ. Press, 2004.

[26] S. Boyd, L. Xiao, A. Mutapcic, and J. Mattingley, "Notes on decomposition methods," Stanford Univ., Stanford, CA, USA, Note EE364B, 2007, pp. 1–36.

[27] D. P. Bertsekas, *Nonlinear Programming*. Belmont, Ma, USA: Athena Scientific Belmont, 1999.

[28] A. H. Phan, H. D. Tuan, H. H. Kha, and D. T. Ngo, "Non-smooth optimization for efficient beamforming in cognitive radio multicast transmission," *IEEE Trans. Signal Process.*, vol. 60, no. 6, pp. 2941–2951, Jun. 2012.

[29] T. Lipp and S. Boyd, "Variations and extension of the convex–concave procedure," *Optim. Eng.*, vol. 17, no. 2, pp. 263–287, 2016.

[30] Fujii Laboratory. *Nagoya University Multi-View Sequences Download List*. Accessed: Mar. 10, 2019. [Online]. Available: http://www.fujii.nuee.nagoya-u.ac.jp/multiview-data/

Wei Xu received the B.E. degree from Hangzhou Dianzi University, China, in 2017. He is currently pursuing the master's degree with the Department of Electronic Engineering, Shanghai Jiao Tong University, China. His research interests include multi-view video transmission and convex optimization.

Ying Cui (S'08–M'12) received the B.E. degree in electronic and information engineering from Xi'an Jiao Tong University, China, in 2007, and the Ph.D. degree in electronic and computer engineering from the Hong Kong University of Science and Technology (HKUST), Hong Kong, in 2011. From 2012 to 2013, she was a Post-Doctoral Research Associate with the Department of Electrical and Computer Engineering, Northeastern University, Boston, MA, USA. From 2013 to 2014, she was a Post-Doctoral Research Associate with the Department of Electrical Engineering and Computer Science, Massachusetts Institute of Technology (MIT), Cambridge, MA. Since 2015, she has been an Associate Professor with the Department of Electronic Engineering, Shanghai Jiao Tong University, China. Her current research interests include optimization, cache-enabled wireless networks, mobile edge computing, and delay-sensitive cross-layer control. She was selected to the Thousand Talents Plan for Young Professionals of China in 2013. She was a recipient of the Best Paper Award at IEEE ICC, London, U.K., June 2015. She serves as an Editor for IEEE TRANSACTIONS ON WIRELESS COMMUNICATIONS.

Zhi Liu (S'11–M'14) received the B.E. degree from the University of Science and Technology of China, China, and the Ph.D. degree in informatics from the National Institute of Informatics.

He was a Junior Researcher (Assistant Professor) with Waseda University and a JSPS Research Fellow with the National Institute of Informatics. He is currently an Assistant Professor with Shizuoka University. His research interests include video network transmission, vehicular networks, and mobile edge computing. He is a member of IEICE. He was a recipient of the IEEE StreamComm2011 Best Student Paper Award, the 2015 IEICE Young Researcher Award, and the ICOIN2018 Best Paper Award. He has been serving as the chair for a number of international conference and workshops. He is/has been a Guest Editor of journals, including *Wireless Communications and Mobile Computing*, *Sensors*, and *IEICE Transactions on Information and Systems*.